A FLIGHT SIMULATION FACILITY FOR MANUAL CONTROL STUDIES

A Thesis Submitted

In Partial Fulfilment of the Requirements

for the Degree of

MASTER OF TECHNOLOGY

by

Sqn. Ldr. C.N. Seshadri

to the

DEPARTMENT OF ELECTRICAL ENGINEERING
INDIAN INSTITUTE OF TECHNOLOGY KANPUR

August 1972

CERTIFICATE

Certified that this work on "A Flight Simulation Facility for Manual Control Studies" has been carried out under my supervision and that this has not been submitted elsewhere for a degree.

P. Ramakrishnarao.

Dr. P. Ramakrishna Rao
Assistant Professor
Department of Electrical Engineering
Indian Institute of Technology
Kanpur

ACKNOWLEDGEMENT

The author wishes to record his deep sense of gratitude to Dr. P. Ramakrishna Rao for the constant advice and guidance given without which the work could not have been completed. His advice was indeed invaluable during the assessment of the case studies performed. The author is indebted to Dr. U.R. Prasad for suggesting an interesting topic and giving valuable advice during construction of the simulation facility. Thanks are due to Shri N.J. Rao for useful suggestions during construction of the facility and to Shri M.S.Krishnamoorthy and Shri C.V.R. Murthy for valuable discussions on case studies performed. Thanks are also due to Shri S.P. Chakrabortty of the Analog Computer Laboratory for his ready help during simulation work. The author is grateful to the staff of Electrical Engineering Dept., Central Workshop, Flight Laboratory of Aeronautics Department and his Air Force colleagues at A.F. Station Kanpur for the assistance rendered. Finally the author thanks Mr. K.N.Tewari for his excellent typing of the thesis.

TABLE OF CONTENTS

LIST OF TABLES

LIST OF FIGURES

LIST OF PHOTOGRAPHS

ABSTRACT

In aviation field, a rudimentary flight simulator is a handy tool for validating theoretical results or models, studying man machine system performance, cockpit display comparisons and the like. One such facility built, has been described in this thesis along with the illustrative studies performed on the facility.

The simulation assembled consisted of a controller similar to a fighter aircraft, a symbolic display unit, a bank of analog computers and peripheral units. The controller enables a realistic pitch axis control and symbolic 3 axis control. The display, though symbolic, has flexibility in use. The analog computers used were EAI type TR 20 and hence have extensive scope for nonlinearities. The peripheral units were mainly EAI X-Y recorders and Brush paper tape recorders.

Two case studies were taken up as illustrations. The first was a display optimisation study for aerial combat. A typical aerial pursuit evasion problem, solved using differential game theory was simulated on the analog computer. The evader was programmed optimal in the computer while the human pilot took the role of pursuer. Three subjects were tried, first a test pilot, next an average fighter pilot and the third an engineer with a flying background. The pursuer was presented state variable displays,

two types of quickened variable displays and an optimal control display. Though the last one made the pilot's task easy, it was found very sensitive to system errors with the pilot having no control over it. The quickened variable displays with a reasonable correlation to the pilot's control outputs enabled consistent performance by the pilots. This tallied with the results of Sheldon Baron.

The second was a pilot model validation study. An attempt was made to use the validated model to decide an aircraft longitudinal design parameter. The pilot model was generated using optimal control theoretic considerations. The model was realised on the analog computer along with the input model and plant dynamics. The performance was studied for various weightages of the components of the performance index. The performance of an experienced pilot was then found to be near optimal and it exhibited close similarity with a particular model. The identified model was reasonably close to that arrived at by Mcruer . Using this performance index, pilot runs of the simulator were done for various pitch damping ratiosof a VTOL aircraft in hover. The variation in performance index gave an indication of the range for choice of the damping ratio. The best value for damping ratio determined by Lollar experimentally was found to lie in this range.

CHAPTER 1

INTRODUCTION

1.1 GENERAL

In the field of aviation, it is important that all systems designed be compatible with the human pilot. This compatability is often investigated by a judicious combination of analysis and experimentation. The machine model used for the experimentation is known as a 'flight simulator'. The simulators are also useful as training devices for the human pilots.

1.2 A TYPICAL FLIGHT SIMULATOR

A flight simulator basically consists of a cockpit with audio visual and/or motion cues and a computation scheme with performance recorders. A block diagram of a typical piloted flight simulator[1] is shown as Figure 1.1. What is done in the simulator is to present the problem to the pilot experimenter in such a form that he can identify and assess its specifics, and give us a subjective rating of his ability to carry out the analagous problems in flight. One must also be able to represent the response characteristics of the controlled element and to vary them at will. It should be possible to control those factors represented by extravehicular disturbances. The vehicle response quantities must be fed back to the operator in

such a way as to readily indicate the status of the vehicle and to provide necessary cues for conducting the required task.

1.3 TYPES OF FLIGHT SIMULATORS

Depending on the facilities available in the simulator, they are classified as rudimentary, basic and advanced simulators.[1] Each of these types can be specific to a particular aircraft or of a nature suited for different general studies. The rudimentary simulator is more meant for qualitative studies and part tasks. They are fairly simple with fixed base control facility and symbolic displays. The basic simulators are a bit more sophisticated with more realism and representative nonlinearities. They could be fixed base or may have facilities for motion cues. The advanced flight simulators are complete representatives of an aircraft with audio visual and motion cues. The displays involve all phases of flight requirements and are as comprehensive as in an aircraft with provision of even system failure simulation facilities. A complete mission from start up to switch off can be simulated in these. These could be specific aircraft oriented or function oriented. Examples of the former are Boeing 707 simulators available with most of the commercial airlines all over the world and of the latter is the air-to-air combat simulator at LTV Aerospace Corporation, U.S.A.[4] A detailed classification as described by Belsley is given in Table 1.1.

1.4 APPLICATIONS OF FLIGHT SIMULATORS

Depending on the complexity of the simulator and facilities available the simulators find wide applications. An effort is made to give some idea of the possible uses of the simulators.

1.4.1 Development of Human Pilot Models

The flight simulator has frequently been used as a basic research tool to develop and test qualitative and quantitative models for human pilot. The comprehensive work by Duane T. Mcruer bears testimony to this. After long years of work at Flight Control Division of U.S. Airforce Flight Dynamics Lab. and NASA Ames Research Center widely accepted and validated quasilinear models for human pilots have been developed[17]. Apart from an interest in quantitative models, the developed man-machine models could be used for analysis, reducing the need for empirical investigations.

1.4.2 Feasibility Demonstrations

Flight simulation can be used for system or subsystem feasibility demonstrations, feasibility studies of new control problems and techniques. They could also be used to delineate potential control problem areas. Effectiveness of various controls like the bang-bang and proportional control to the pilot can be assessed. In many cases it has been possible to use flight simulation

as a preliminary design test to demonstrate or eliminate specific guidance techniques. R.W. Obermeyer gives examples of the study of manual control of large space boosters and manual lunar landing studies[2].

1.4.3 Comparative Studies in System Design

Flight simulators are often used for system or sub-system comparison studies. These can be in terms of selection/choice of effective display parameters or may involve hardware comparisons of different display facilities for any particular system parameter or even comparing types of controllers. The first is useful in the preliminary design of vehicle systems while the other two help in choosing the best possible realisation of the system hardware. An example of the controller selection is the study done in Boeing Laboratories[5]. For guidance and control this is perhaps the most common application for simulators.

1.4.4 Handling Qualities Investigations

Early in the development of manual control systems, judgement of the pilot was found to be essential in evaluating the acceptability of a given control system. These so called 'handling qualities requirements' define acceptable handling qualities for flight vehicles. Flight simulators are used to evolve synthetic handling qualities criteria which can be used for preliminary system design and experimentation without the presence of a pilot. Later

the synthesised system can be individually checked out by the pilot on the flight simulator and classified under accepted handling quality ratings.

1.4.5 Total System Performance Evaluation

The advanced flight simulators make it possible to have full mission investigations and total system performance. The behaviour of the aircraft for any particular mission can be fully tested out on the simulator. These could be of particular value when the missions are of a military nature with dangerous consequences if mission fails.

1.4.6 Aircraft Comparison for a Specific Role

The simulators if sophisticated but of a general nature, can be used to assess relative performance of different aircraft for a particular role. An example is the manned air-to-air combat simulator in LTV Aerospace Corporation, USA.[4] Here an aerial combat canbe fully simulated and relative performance of say two fighter aircraft pitted against each other can be assessed. By varying the aircraft parameters possible improvements to aircraft can be assessed.

1.4.7 Flight Training

Another obvious use of a flight simulator is in pilot training. Operational training on aircraft is rather

costly both in terms of cost involved in each aircraft sortie and risks involved for inexperienced pilots. A flight trainer becomes a handy tool. Indian Air Force experience indicates that practice missions by inexperienced pilots first on the trainer simulators greatly reduce the actual operational training required to be given. Further the pilots also can be given full training in reacting correctly during mission emergencies like fire in the engine or specific system failures.

1.5 CHOICE OF SIMULATOR

Choice of the type of simulator to be assembled would mainly depend on two factors. First to be considered are the objectives of the experiments to be performed and next come the availability of resources.

The first phase, in the building of a flight simulation facility, is then, the decision on the types of experiments to be performed and the nature of results expected. This study is best done by a team consisting of the designer and the operator (pilot). Dependent on the nature of the results expected and areas of their application, the complexity of the simulator will be decided. The complexity required would indicate the type of simulator to be acquired.

Having arrived at the complexity of the simulation facility, an assessment of the resources is to be made.

Depending on the resources, the complexity planned may have to be pruned. This reverse process will then indicate the scope of the simulator. With this, one is ready for building the simulator.

Next stage is setting up on the analog/digital computers, the equations of motion/software of the system to be used. The equipment to provide both the vehicle response computation and response feedback information must be assembled and checked out. At this stage, the overall simulation scheme must be validated by the operator to bridge the gap between real life situation and the simulator situation. If necessary, modifications should be made to the simulation set up or a reduction of objectives can be made. Such was the process gone through in building a facility to analyse basic flight control problems. Specific areas of interest at the outset were a) Human pilot models and b) Study of aerial combat situations, with a view to decide on the most efficient display patterns for the pilots.

As the results expected were more qualitative in nature, a general fixed base type of simulator was decided upon with only symbolic displays. To provide suitable environment to the pilots to be used for the aerial combat study, it was decided to make the cockpit controllers, as in a jet fighter aircraft. However, due to the non-availability of components readily, it was decided to have

symbolism even in the controls. Rudder control was hence avoided. A throttle and a joystick were accepted as the control mediums for the pilot. Again due to the qualitative nature of the results expected the accuracy of an analog computer was acceptable with X-Y recorders forming the main devices to measure the performance.

The chapter that follows, gives a detailed description of the flight simulation facility. Two case studies done,, one regarding a pilot model based on modern control theory and the other an optimum display study for aerial combat, have then been described in detail. The thesis ends with a discussion of the results obtained and suggestions for future work.

	Rudimentary	Basic	Advanced	Advanced
Application	Determining 1st order requirements for controllability about and of the flight path; Feasibility studies of new control problems and techniques; Delineation of potential control problem areas.	Gross Handling Quality trends; Defining boundary spaces; Determining 1st order interrelationship between modes of motion and control of and about the flight path; Cockpit display developments.	Minimum acceptable handling qualities; Defining operational problems; Navigational and guidance problems; Cockpit display effectiveness.	Overall operating problems - definition and solution; Certification problem; Definition of minimum acceptable handling qualities; Display aids analysis.
Results	Qualitative (Quantitative if sufficient elements of problem included)	Qualitative	Qualitative (Relatable to flight)	Qualitative (Directly applicable to flight)
Task complexity	Generally part task	Part task (Pilot initiated short term tasks involving discrete parts of problem)	Whole task (specific operational-longer term tasks including greater percentage of problem).	Whole task (complete mission capability)
Sophistication and realism	Minor..... (Symbolic display) No motion.	Increasing computational complexity and degrees of freedom....Maximum feasible (Basic inst.only) (Ext.visual display and motion if avail.)	(More complete cockpit inst. Ext.visual display and motion as required)	(Most complete representation of vehicle
Method of evaluation	Subjective pilot opinion from pilot initiated tasks	Primarily subjective pilot opinion from pilot initiated tasks.	Subjective pilot opinion plus task performance, longer term.	Primarily task performance based on fairly complete criteria plus subjective pilot opinion.

TABLE 1.1: CLASSIFICATION OF PILOTED SIMULATORS.[1]

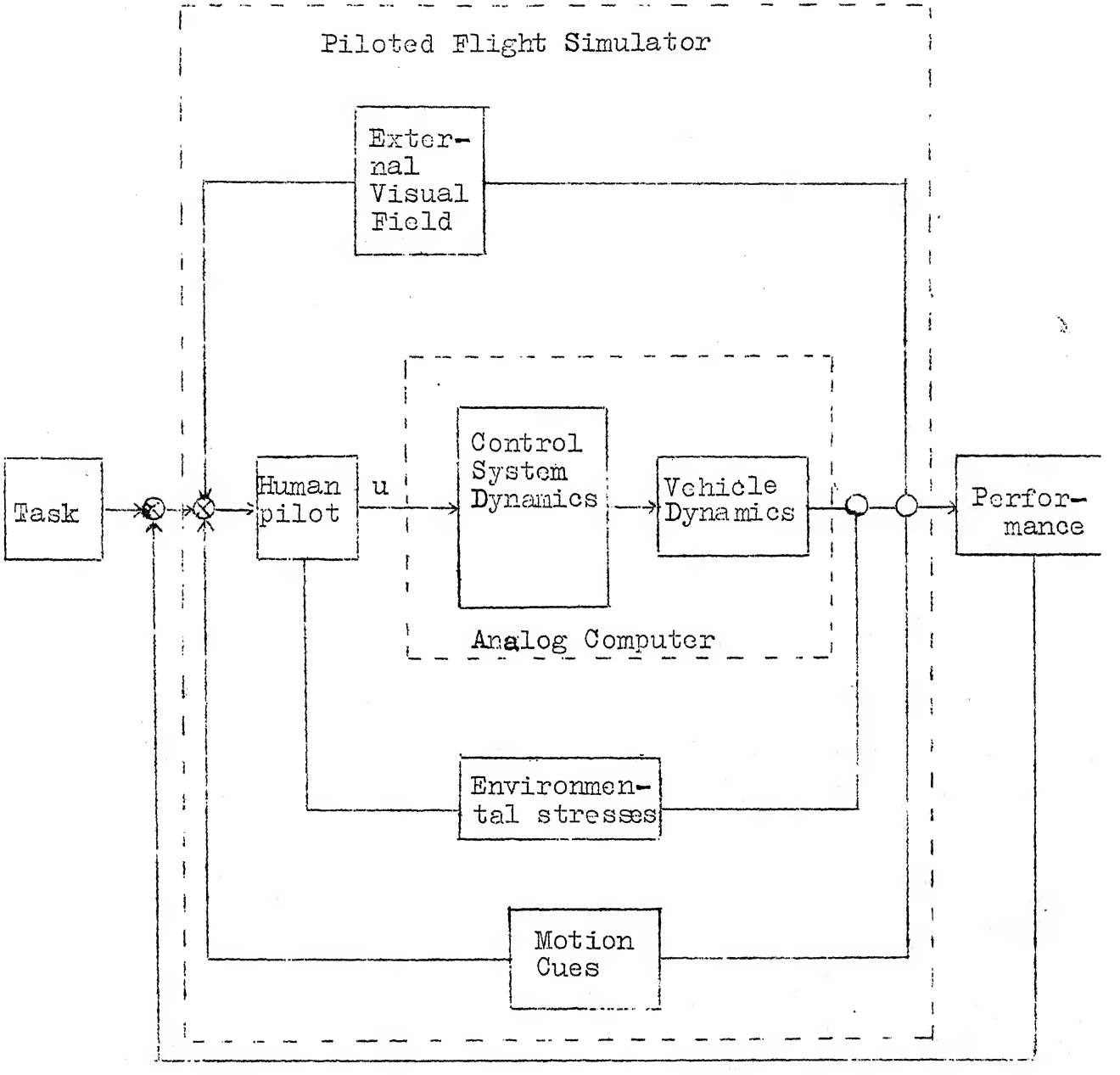

FIG.1.1: BLOCK DIAGRAM OF PILOTED FLIGHT SIMULATOR.

CHAPTER 2

FLIGHT SIMULATOR: A DETAILED DESCRIPTION

2.1 INTRODUCTION

An overall view of the flight simulation set up assembled, is shown in photograph no.2.1. This would conform to the class of rudimentary flight simulators discussed in Chapter 1. In an actual flight, the aircraft is flown by a pilot sitting in the cockpit and controlling the movements of the flight vehicle through the main controls of control stick, rudder and engine throttle. The effects of his control actions are fed back to him in terms of the flight status of the aircraft in atmosphere and in instrument flight conditions, by the instrument displays available to him. In the simulator the pilot sits in the simulated cockpit and controls the system through similar controls as in aircraft. His movements are, however, converted into electrical signals and fed into the analog computers on which the complete system is simulated. The analog outputs are presented to the pilot as an instrument display, indicating the effects of his control actions.

In the simulator built, full realism is available only for movements in pitch axis, through throttle and the control stick. For other types of study the controls give, in the absence of rudder pedals, a symbolic three axis control. In this mode, the control stick could be used to

give control for vertical and lateral movements. The throttle can be assumed to effect the longitudinal movement.

2.2 BLOCK DIAGRAM

A block diagram of the facility is given in Figure 2.1. The simulator can be briefly grouped into three assemblies. The first is the simulator cockpit consisting of the pilots control components and the display unit or the instrument panel. The pilots sits in an aircraft seat provided for him on the simulator, gives out his system control actions through the set of controls available and amends his control actions with the cue available from the visual display panel. The next is the analog computer bank. This processes the pilot outputs through the system equations and feeds to the pilot's display unit the existing status of the system. The third is the performance recording unit which is used as such, through the use of X-Y recorders and paper tape recorders.

2.3 COCKPIT CONTROLLER

2.3.1 General

The external view of the controller is seen in photograph 2.1. The controller is assembled on a wooden base and is covered by a wooden case which forms the floor of the rudimentary cockpit. Sticking out of the floor are

the control column and the throttle. These controls surround a comfortable aircraft seat.

2.3.2 Controller Specifications

Relative positions of the controls with respect to the pilot's seat are indicated with dimensions in Figure 2.2. To ensure easy adaptability of the subject pilots, the control stick and the throttle were identical to those fitted on a jet fighter aircraft. The control column hand grip has a diameter of 1.4". This is in conformity with a widely accepted range[9] of 1.375"to 1.685". The distances between the pilot's seat and the controls were adjusted to be nearly same as in a modern jet fighter aircraft.[8] However, the seat itself was kept movable to suit individual requirements of each pilot. The extent of movement of the control stick in longitudinal and lateral dimensions as well as the longitudinal movement of the throttle was kept adjustable depending on the type of study conducted. For the illustrative studies described in Chapters 3 and 4, the specifications maintained were as indicated in Table 2.1. These were similar to those specified for a jet fighter aircraft current ly in use.[6] The artificial feel loadings on the control was kept as mentioned in Table 2.1. The loadings were kept at half the value used in a light jet fighter aircraft[7] so as to avoid muscular fatigue on the pilot doing the repeated

simulator runs required for the experiments. The subject pilots felt the feel to be comfortable.

2.3.3 Constructional Features

2.3.3.1 A perspective diagram of the controller sub-assembly is given in Figure 2.3. The controller is fully covered by a wooden case which forms the floor of the symbolic cockpit and through which only the control stick handle and throttle handle stick out. In the aircraft, movements of the controls cause corresponding mechanical movement of relevant control surfaces. In the simulator the same movements produce electrical signals corresponding to the movements of the controls which are given as inputs to the analog computer system. These electrical signals were generated by linking the movement of potentiometer wipers with those of the controls. The two ends of the wire wound potentiometers were connected to +10V and -10V d.c. supply points so that the potentiometer wipers pick off positive and negative d.c. values depending on the control position.

2.3.3.2 Longitudinal movement of control column:

The control column has a transverse torque tube at the lower end. To each end of this torque tube is fixed a double ended lever. Lower ends of these levers are connected to the floor mountings permitting fore and aft movement about these points. The upper end of the

left lever transmits the movement of the column to a quadrant pulley through a connecting rod. The quadrant pulley has a potentiometer connected to its axle. The stem of the potentiometer rotates with the quadrant pulley and thus generates an electrical signal proportional to the fore and aft movement of the stick.

To limit the movement of the stick, two limit stops are fitted controlling the movement of the double ended lever. The loading on the stick is provided by artificial feel units attached to the quadrant pulley. To ensure realism the feel units were identifal to the ones fitted on a modern transonic fighter aircraft. These feel units consist of two graded springs (Figure 2.4).

2.3.3.3 Lateral Movement of control column:

The grip handle of the stick is integral with a sprocket which is connected through tie rods and chain to another sprocket wheel at the bottom of the control stick (Figure 2.5). This sprocket wheel is attached through an universal joint to a circular pulley. A potentiometer is kept aligned with the axis of the pulley. Lateral movement of control column handle is converted thus as a rotary movement of the pulley and potentiometer wiper. Stops for the lateral movements are provided on the bottom sprocket wheel and loading for lateral movement

is ensured by an artificial feel unit similar to the one for fore and aft movement, connected to the circular pulley.

2.3.3.4 Throttle movement:

For this, a throttle identical to that fitted on a jet fighter aircraft was used. The throttle feel was given by the frictional mounting of the unit. Adjustable stops were provided for the throttle. To the axis of the throttle handle was attached a potentiometer which picks off signals corresponding to the throttle position.

2.3.4 Adjustments for Controllers

The following adjustments are available on the controller intended for flexibility in use:

a) Adjustable arc of movement for control column, longitudinally and laterally.
b) Variable stick loading, longitudinal and lateral.
c) Adjustable arc of movement for throttle.
d) Variable loading of throttle.

2.3.4.1 Arc of movement - control column:

The maximum fore and aft movement of the control stick (arc of movement) is controlled by the continuous stops on the double ended lever of the torque tube as indicated in Figure 2.6(a). The stop consist of brackets fitted with threaded bolts. The top stop bracket is attached to the floor mounts, and a bolt is fitted on the

bracket which can be moved up or down. This acts as a stop on the lower arm of the double ended lever. Bottom stop bracket is clamped to the floor using two bolts. A third bolt acts as the lower stop as shown in Figure 2.6(a). The arc of movement of the control column laterally is limited by using variable size stops. These stop the movement of the stop plate, attached to the lower sprocket wheel indicated in Figure 2.5.

2.3.4.2 Variable stick loading for longitudinal and lateral movements:

These arrangements are similar in both lateral and longitudinal directions. The artificial feel unit is attached to the circular pulley (or quadrant pulley for longitudinal) through an adjustment plate with one ordinary hole and an elongated hole. The adjustment plate is fixed with two bolts to the circular pulley . The stem of the artificial feel unit is clamped to the adjustment plate through the elongated hole. The loading on the stick can be varied by shifting the attachment point of the AFU stem along the elongated hole(Figure 2.6(b)).

2.3.4.3 Adjustable movement of arc and loading-throttle:

The adjustment in the arc of movement is achieved by change of position of the stops indicated in Figure 2.6(c). The throttle friction loading is controlled by the tightness of the loading adjuster clamp which causes the throttle

friction plates to be held tightly by the two arms of the throttle stand. While the throttle is moved, the friction plates move with respect to the sides of the throttle stand arms (Figure 2.6(d)).

2.4 DISPLAY UNIT

This unit was essentially symbolic in nature. The display unit can be seen in the photograph 2.1. The unit consisted of d.c. voltmeters and oscilloscopes fitted in a display panel enclosed in the display box. A cable bunch bringing input to the meters has an entry at the rear. The cables of the display unit were marked serially and were connected to a display connector box. The display panel was made in such a way that the panel can easily be removed by unscrewing four screws, when the display pattern and layout were to be changed. The voltmeters were used for representing symbolically various flight parameters like energy left, closing speed of aircraft, etc. Two oscillators one of Tetronix 503 and another Tektronix 310A type were used to display state vector or control vector display.

2.5 ANALOG COMPUTATION BANK AND PERIPHERAL UNITS

The computer assembly forms the brain of the flight simulator. The assembly consists of a bank of three EAI analog computers type PACE-TR 20 and one 'EXACT' function generater type 340. The three TR 20 computers are kept slaved and are hence operated as a single unit

for all practical purposes. The computer assembly with a few recorders attached to it can be seen in photograph 2.2. The specifications for the computing elements are placed at Appendix A.

A function generator type 240 was used in conjunction with the relay comparator of TR 20 set to provide beam splitting facility for oscilloscope display. A 30 cycles per second sinusoidal signal of 6V peak to peak is fed from the function generator to the 'IN 1' terminal of the relay comparator. 'IN 2' terminal is fed with -1V supply. The added input to the relay comparator energises and deenergises the relay approximately 60 times a second causing the relay contacts to change over accordingly. This results in the input to the oscilloscope being alternately selected from two different sources. Due to persistence of trace on the scope, two traces appear corresponding to the two inputs.

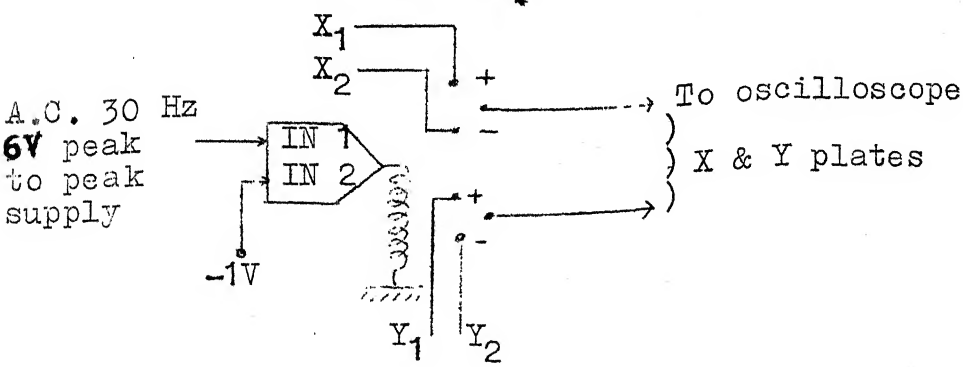

Figure 2.7

The peripheral units of the flight simulator make available permanent recordings of the pilot performance parameter variations. For the simulation facility assembled this peripheral group consisted of

a) Two EAI X-Y recorders

b) One MOSELEY X-Y recorder

c) One 'Brush' strip chart recorders.

2.6 CONCLUSION

It can be seen that the flight simulation facility built was a rudimentary one with symbolism in display and control. However, it was simple in structure and used components familiar to a professional pilot. This leads to easy adaptation by the subject pilots during experimentation.

Table 2.1

CONTROLLER SPECIFICATIONS

Component	Specification	
Control Stick	Longitudinal arc of movement	: 22° fwd. 13° aft
	Lateral arc of movement	: 30° eitherway
	Longitudinal load	: 0 - 8 lbs. fwd. 0 - 15 lbs. aft. 0.5 lb breakout.
	Lateral load	: 0 - 7 lbs eitherway 0.5 lb breakout
Throttle	Arc of movement	: 10° from Rear to vertical 40° from vertical to full forward.
	Loading	: 5 lbs. uniform.

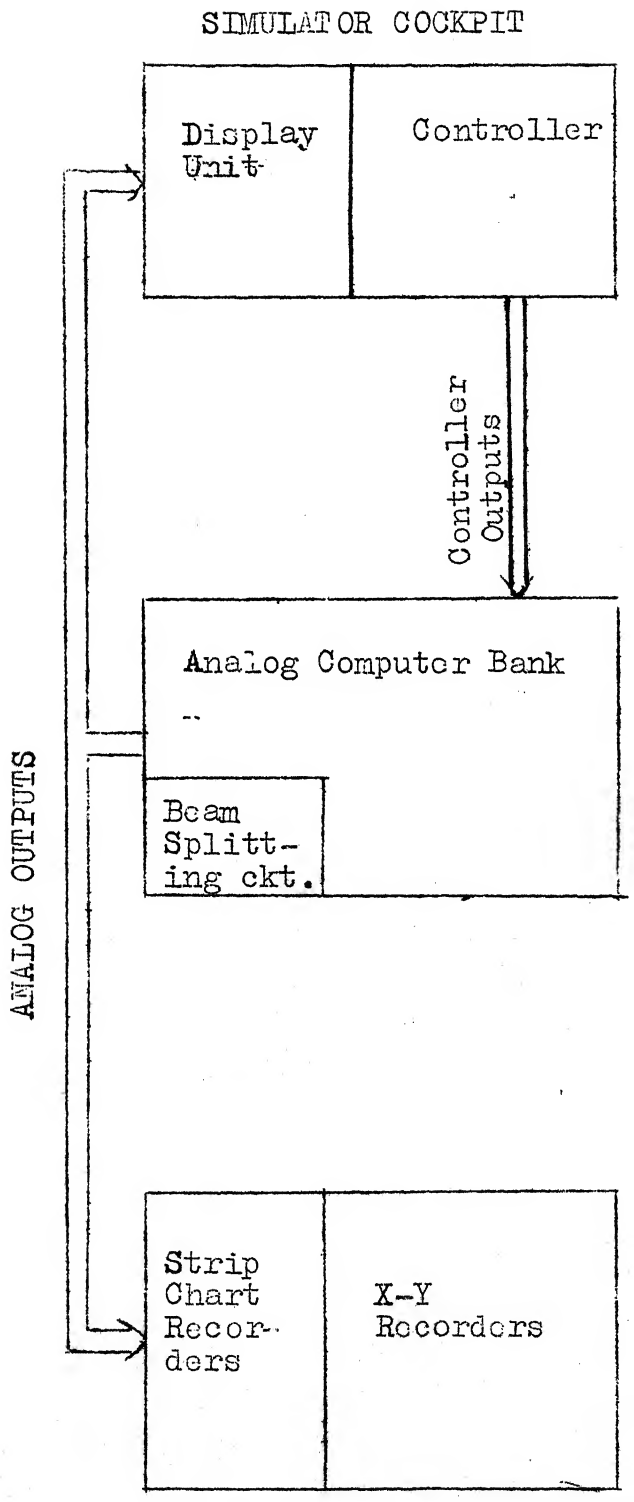

FIG.2.1. BLOCK DIAGRAM OF SIMULATION FACILITY

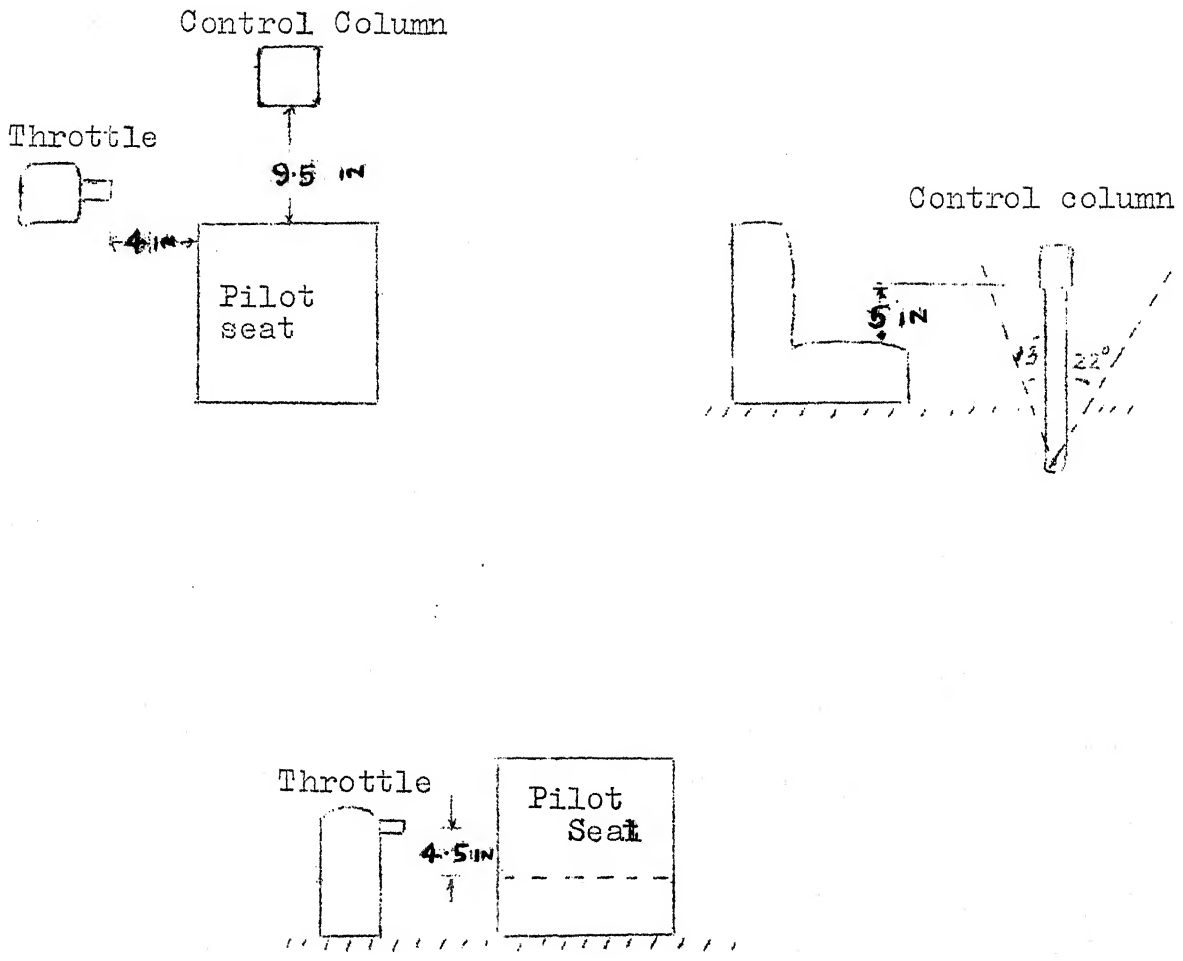

FIG. 2.2 RELATIVE POSITIONS OF CONTROLS.

LAYOUT OF CONTROLLER

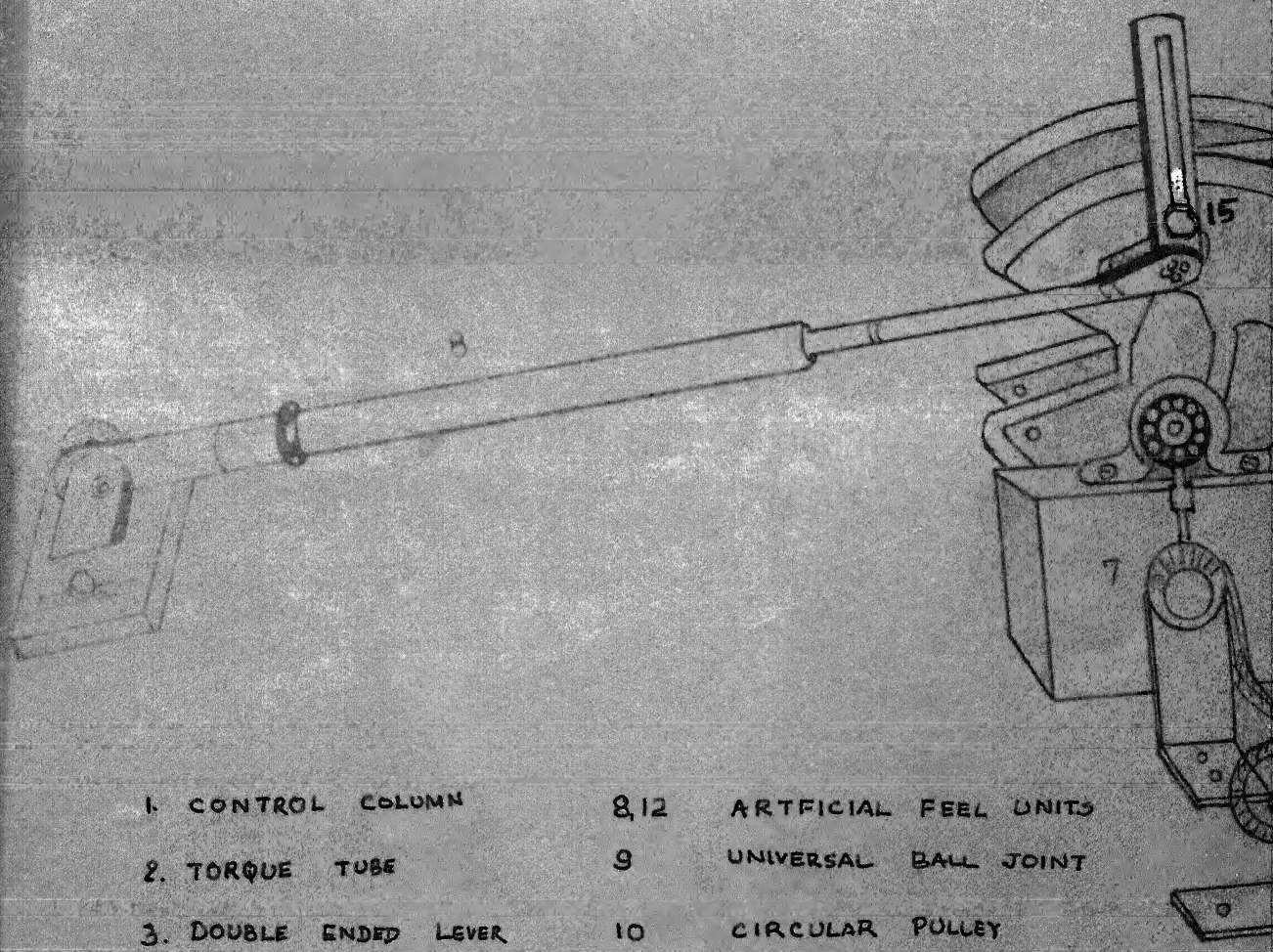

1.	CONTROL COLUMN	8,12	ARTFICIAL FEEL UNITS
2.	TORQUE TUBE	9	UNIVERSAL BALL JOINT
3.	DOUBLE ENDED LEVER	10	CIRCULAR PULLEY
4,5	LONGITUDINAL STOPS	13	THROTTLE STAND
6	QUADRANT PULLEY	14.	THROTTLE HANDS
7,11	POTENTIOMETERS	15,16	ADJUSTMENT PLATES FOR STICK

FIGURE. 2.3

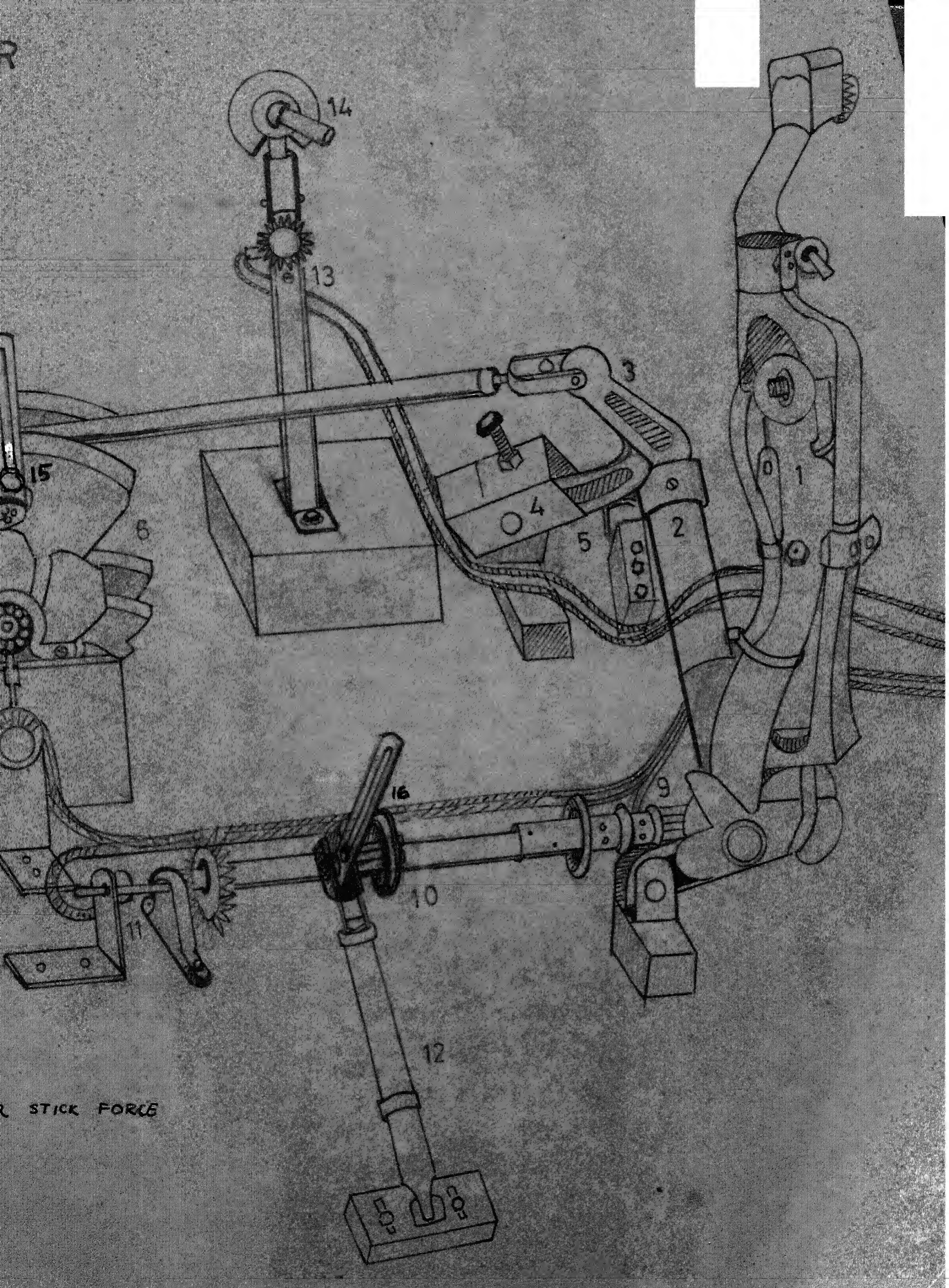

STICK FORCE

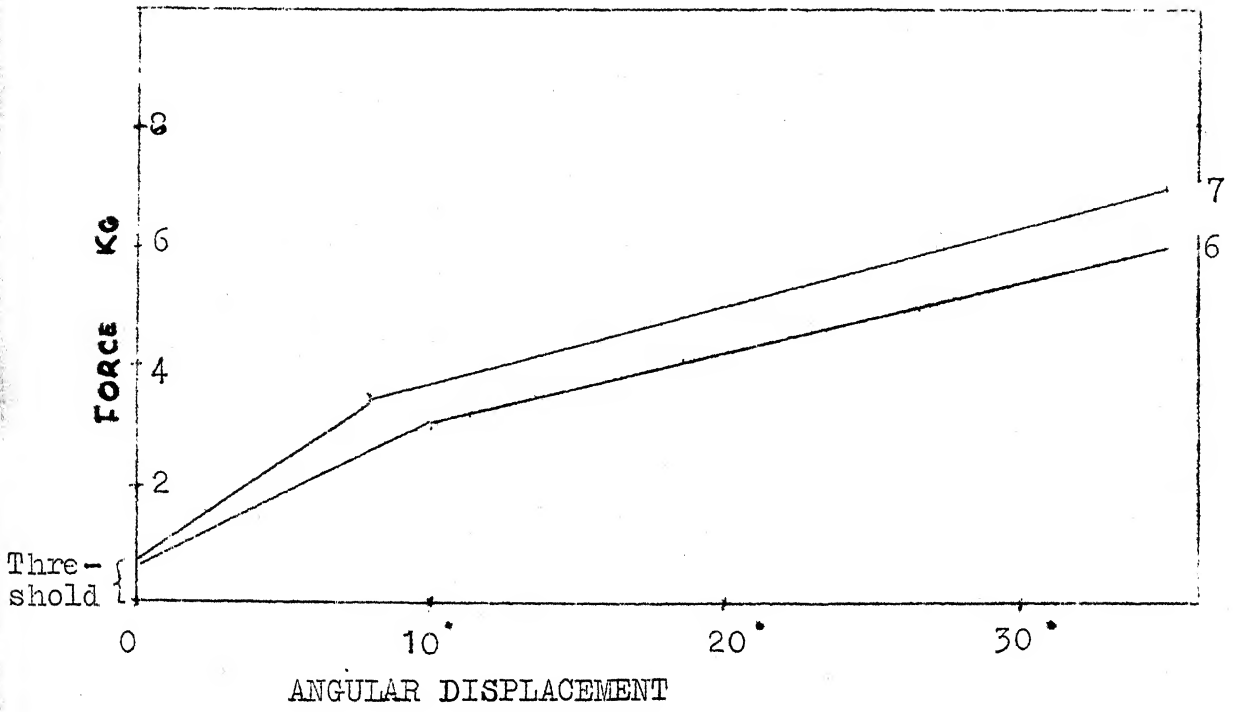

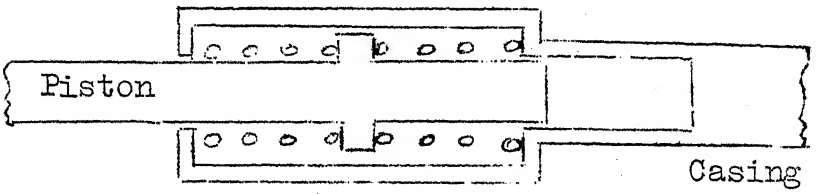

FIG.2.4 ARTIFICIAL FEEL UNIT

CONTROL COLUMN-REAR VIEW

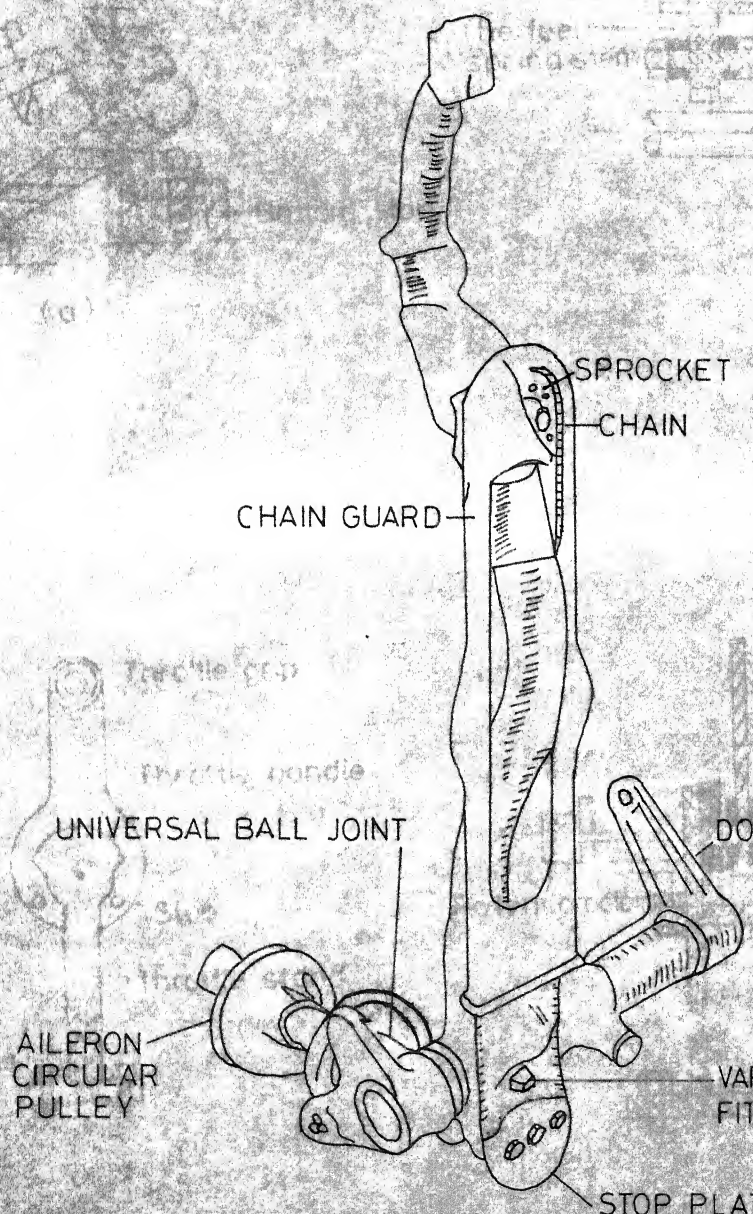

FIG. 2·5

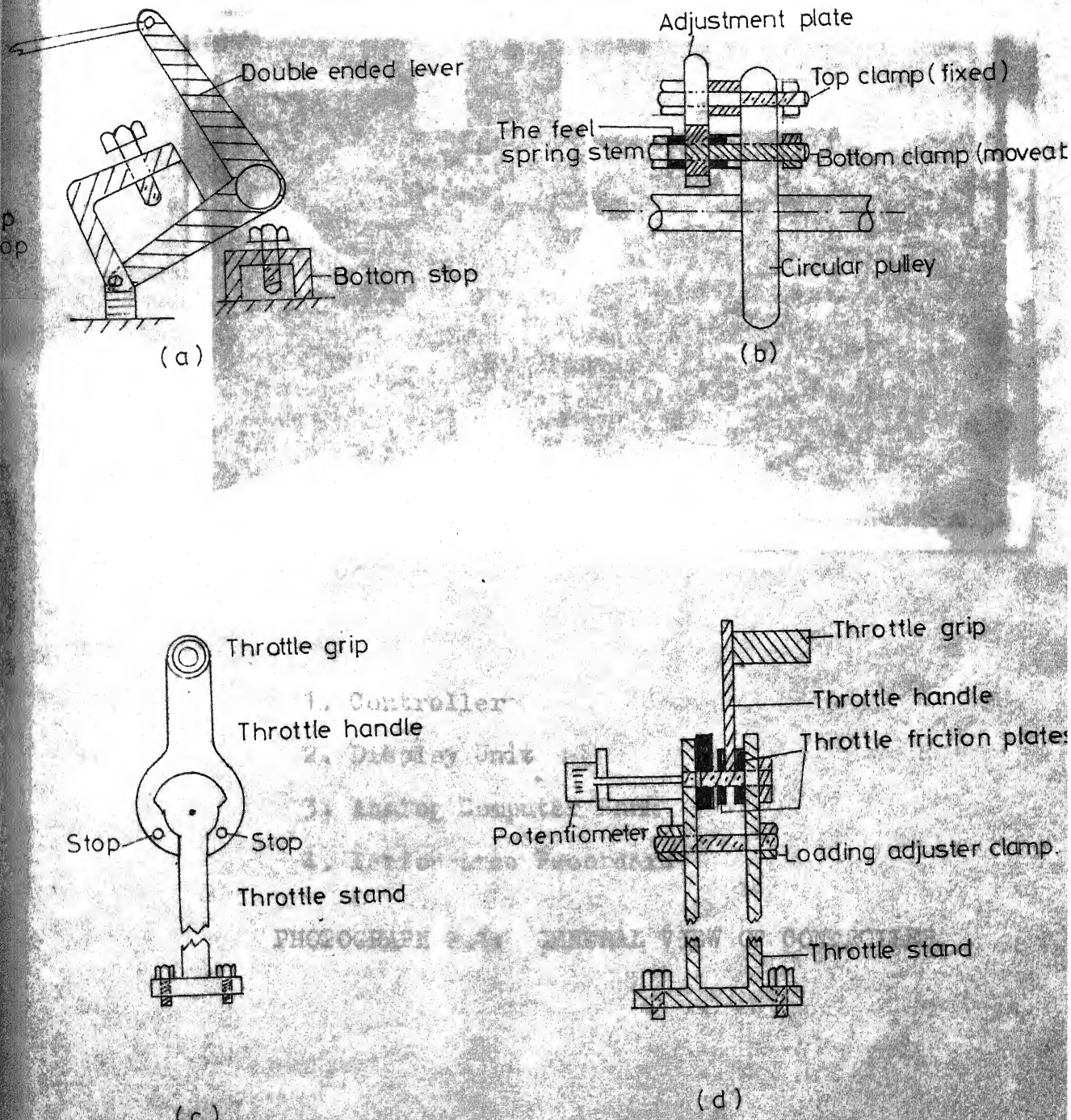

FIG. 2·6 CONTROLLER ADJUSTMENTS

1. Controller
2. Display Unit
3. Analog Computer Bank
4. Performance Recorders

PHOTOGRAPH 2.1: GENERAL VIEW OF CONTROLLER

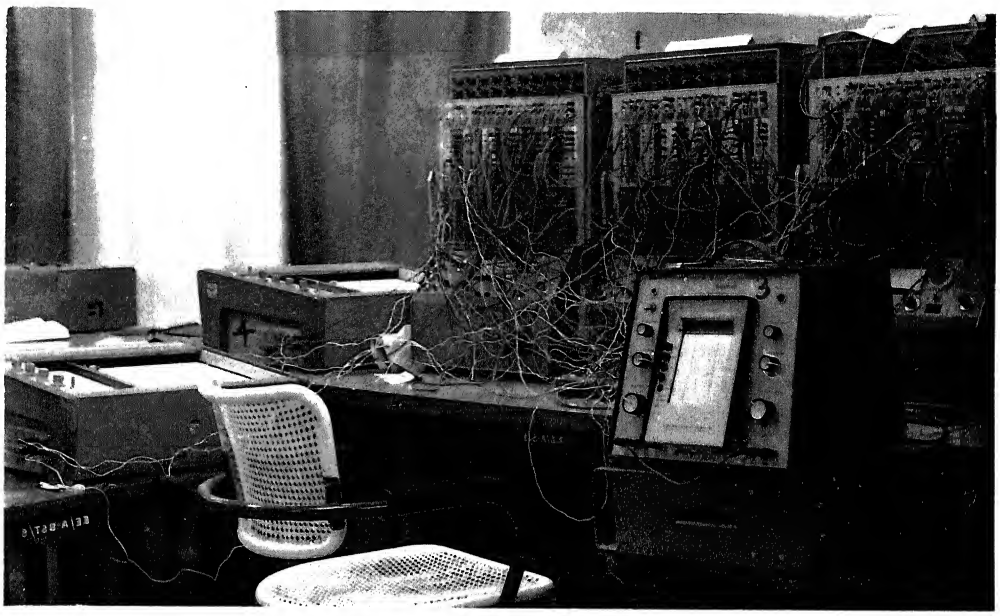

1. Analog Computer with Setup
2. Function Generator for Oscilloscope Beam Splitting.
3. 'Brush' Strip Chart Recorder.
4. 'EAI' X-Y Recorders.

PHOTOGRAPH 2.2: ANALOG COMPUTER AND PERFORMANCE RECORDERS, SETUP FOR CASE STUDY 1

CHAPTER 3

CASE STUDY NO.1: OPTIMAL DISPLAY IN AERIAL PURSUIT EVASION

3.1 OBJECTIVE

To simulate an aerial pursuit evasion game, study the performance of a human controller (pilot) for different display parameters and ascertain the nature of the most efficient display.

3.2 STUDY PROCEDURE

A meaningful pursuit evasion problem was chosen as a first step. The problem dynamics were patched up on the analog computer. The solution to the problem was fully generated with the minimum use of the computing elements. A feedback loop with human pilot in it was then programmed. The human controller was given the task of minimising (or maximising) the distance between the pursuer and evader at the end of a fixed time corresponding to the human pilot's role of being the pursuer (or evader).

In this task, the human controller was given progressively different types of display and in each case his performance was recorded. The errors were then calculated. The display giving the lowest (or highest) miss distance with the human pursuer (or evader) was chosen as the best display. Its characteristics were then analysed.

The runs were performed with different subjects to gain more confidence about the results. This also helps to see the adaptability of different subjects to the system.

3.3 PROBLEM BACKGROUND

The problem chosen for simulation is a special class of pursuit evasion differential game solved by Ho, Bryson and Baron in 1965.[11] A differential game may be stated briefly as follows.

Given the payoff

$$J(u,v) = \phi(x(T),T) + \int_{t_o}^{T} L(x,u,v,t)dt \qquad (3.1)$$

and constraints

$$\dot{x} = f(x,u,v,t); \quad x(t_o) = x_o \qquad (3.2)$$

$$u \in U \qquad v \in V \qquad (3.3)$$

determine the pair of feedback controls

$$u^* = \bar{k}(x(t),t) \in U$$
$$v^* = \bar{k}(x(t),t) \in V \qquad (3.4)$$

satisfying the relation

$$J(u^*,v) \leq J(u^*,v^*) \leq J(u,v^*) \qquad (3.5)$$

for arbitrary $u \in U$, $v \in V$.

In game theory, J is called the payoff, x the state of the game and u,v are strategies restricted to certain sets of admissible strategies U,V depending on the problem in question. If strategies u* and v* can be found such

such that (3.5) is true, then they are called pure strategies and the pair (u^*, v^*) is called the saddle point of J. The payoff evaluated at the saddle point, $J(u^*,v^*)$ is called the 'Value' of the game.

The class of problems in which the differential equations are linear, the payoff quadratic and the controls not constrained, was solved using variational methods. A particular case of this, with energy constraints, is considered here.

3.4 PROBLEM STATEMENT[12]

$$\ddot{r}_p = f_p + a_p;\ r_p(t_o) = r_{p_o};\ \dot{r}_p(t_o) = \dot{r}_{p_o}$$
$$\ddot{r}_e = f_e + a_e;\ r_e(t_o) = r_{e_o};\ \dot{r}_e(t_o) = \dot{r}_{e_o} \qquad (3.6)$$

where $r_{p(e)}$ represents the position vector of the pursuer or evader depending on the subscript p or e in 3-dimensional space. 'a' is the control acceleration of the body. It is assumed that the altitude difference between 'p' and 'e' is small and so when we consider the relative position $\underset{\sim}{r}$, the effect of the external forces $\underset{\sim}{f}$ may be neglected.

The equation (3.6) can then be written as

$$\ddot{\underset{\sim}{r}} = a_p - a_e \qquad (3.7)$$

The above equation has implicit in it the state variables r and dr/dt. Now the system state can be expressed in terms of certain predicted or quickened variables also. A new variable is now defined.[12]

$$\hat{r}(t) \triangleq r(t) + (T-t)\,\dot{r}(t) \tag{3.8}$$

This vector can be called the first order predicted miss. Given a relative position and velocity at time t, r(t) and $\dot{r}(t)$, $\hat{r}(t)$ is the relative position which would result at terminal time T if no controls were applied either by the pursuer or evader. Now differentiating (3.8) we get the differential equation in terms of the first order predicted miss as

$$\dot{\hat{r}}(t) = (a_p(t) - a_e(t))(T-t) \tag{3.9}$$

We can also define similarly a second order predicted miss as

$$\hat{\hat{r}}(t) \triangleq r(t) + \int_t^T \dot{r}(t)\,dt \tag{3.10}$$

This would then be the predicted miss at the terminal time T, if from time t, the relative acceleration is kept constant or in other words both pursuer and evader maintained constant control.

Equation (3.10) can be written as

$$\hat{\hat{r}}(t) = r(t) + \int_t^T \{\dot{r}(t) + \ddot{r}(t)\,(T-t)\}\,dt \tag{3.11}$$

where $\dot{r}(t)$ and $\ddot{r}(t)$ are constants for any time t.

After integration, we can write the same as also

$$\hat{\hat{r}}(t) = \hat{r}(t) + \ddot{r}(t)\,\frac{(T-t)^2}{2} \tag{3.12}$$

or still

$$\hat{\hat{r}}(t) = \hat{r}(t) + (a_p - a_e)\,\frac{(T-t)^2}{2} \tag{3.13}$$

The problem now is to determine the saddle point $a_p(t,t_o,r_o,\dot{r})$, $a_e(t,t_o,r_o,\dot{r}_o)$ for a payoff

$$J = \frac{a^2}{2}(r(T).r(T)) \tag{3.14}$$

where $r(T)$ is the relative distance $(r_p(T)-r_e(T))$ at a fixed terminal time T. We see that the payoff is a measure of terminal range for a fixed terminal time T. The objective of the pursuer is to minimise the payoff while that of the evader is to maximise it.

The constraints on the control energy are assumed to be

$$\int_{t_o}^{T}(a_p.a_p)dt \leq E_p^2(t_o)$$

and (3.15)

$$\int_{t_o}^{T}(a_e.a_e)dt \leq E_e^2(t_o)$$

It is obvious that under optimum play the evader will utilise all his energy. It is further assumed for simplicity of analysis that pursuer has just sufficient energy for capture (defined as $r(T) = 0$). With this assumption the constraints become equality constraints and using the Lagrange multiplier technique the payoff is taken as

$$J = \frac{a^2}{2}(r(T).r(T)) + \frac{1}{2}\int_{t_o}^{T}\left[\frac{a_p(t).a_p(t)}{C_p} - \frac{a_e(t).a_e(t)}{C_e}\right] dt \tag{3.16}$$

where $1/C_p$ and $1/C_e$ are the Lagrange multipliers.

Now the solution for this has been derived by Baron [12] as

$$a_p^*(t) = - \frac{E_p(t)}{\sqrt{\frac{T-t}{3}}} \cdot \frac{\hat{r}(t)}{\|\hat{r}(t)\|} \qquad (3.17)$$

and

$$a_e^*(t) = - \frac{E_e(t)}{\sqrt{\frac{T-t}{3}}} \cdot \frac{\hat{r}(t)}{\|\hat{r}(t)\|}$$

where $\|r(t)\| \triangleq (r(t).r(t))^{\frac{1}{2}}$

The corresponding minimax distance is

$$\|r(T)\| \triangleq \|r(t)\| - (E_p(t) - E_e(t)) \frac{(T-t)^3}{3} \qquad (3.18)$$

The energies left at any time t are given by

$$E_p^2(t) = E_p^2(t_o) - \int_{t_o}^{t} \{a_p(t).\, a_p(t)\}\, dt$$

$$E_e^2(t) = E_e^2(t_o) - \int_{t_o}^{t} \{a_e(t).a_e(t)\}\, dt \qquad (3.19)$$

3.5 ANALOG MECHANISATION: SADDLE POINT SOLUTION

A two dimensional version of the above was considered. For simulation on the analog computer and subsequent display on the flight simulator, the above equations have to be resolved into x and y coordinates. The equations required for simulation are (3.7), (3.9), (3.13), (3.17) and (3.19). The solution being in terms of r(t) the equations(3.7) and (3.13) need be used only for visual display and not for solution generation.

The equations (3.19) have to be converted into differential equations for use on analog computer. Substituting for a_p and a_e and converting them to differential equations, we get

$$\dot{E}_p(t) = -\frac{3}{2}\cdot\frac{E_p(t)}{T-t}$$

$$\dot{E}_e(t) = -\frac{3}{2}\cdot\frac{E_e(t)}{T-t} \qquad (3.20)$$

(See Appendix B for details)

Similarly manipulations on equation (3.9) yield

$$\dot{\hat{r}}(t) = \sqrt{3(T-t)}\ \frac{\hat{r}(t)}{\|\hat{r}(t)\|}(E_e(t)-E_p(t)) \qquad (3.21)$$

Now resolving equations (3.7), (3.13), (3.17), (3.20) and (3.21) into x and y coordinates and recognising the symmetry involved in them (See appendix B). We finally get the equations for simulation as

$$\dot{E}_p(t) = -1.5\ \frac{E_p(t)}{T-t} \qquad (3.22)$$

$$E_e(t) = \frac{1}{C}E_p(t); \quad C = \frac{E_p(t_o)}{E_e(t_o)} \qquad (3.23)$$

$$\dot{\hat{r}}_x(t) = \sqrt{\frac{3}{1+k^2}}\left(\frac{1}{C}-1\right)E_p(t)\sqrt{T-t} \qquad (3.24)$$

$$\hat{r}_y(t) = k\,\hat{r}_x(t)\ ; \quad k = \frac{\hat{r}_y(t_o)}{\hat{r}_x(t_o)} \qquad (3.25)$$

$$a_{p(e)_x}(t) = -\sqrt{\frac{3}{1+k^2}}\ \frac{E_{p(e)}(t)}{\sqrt{T-t}}\ ; \qquad (3.26)$$

$$a_{p(e)_y}(t) = k\,a_{p(e)_x}(t) \qquad (3.27)$$

$$\ddot{r}_x(t) = a_{p_x}(t)\ (1-\frac{1}{C}) \tag{3.28}$$

$$\ddot{r}_y(t) = a_{p_x}(t)\ (k-\frac{k}{C}) \tag{3.29}$$

$$\hat{\hat{r}}_x(t) = \hat{r}_x(t) + (a_{p_x} - a_{e_x})\ \frac{(T-t)^2}{2} \tag{3.30}$$

$$\hat{\hat{r}}_y(t) = k\ \hat{\hat{r}}_x(t) \tag{3.31}$$

These equations were mechanised in TR 20 analog computer using analog diagram given in Appendix D. This required the use of two TR 20 computers.

3.6 'PILOT IN LOOP' ANALOG MECHANISATION

In mechanising the feedback loop with the human pilot, it was decided to use the pilot as the pursuer. The evader was considered optimal and was patched on the computer. It was decided to give to the pilot; a) a state variable display, b) a quickened display in terms of $\hat{r}(t)$ c) another quickened display $\hat{\hat{r}}(t)$ and d) control vector display $a_p^*(t)$ to study the relative performance.

The pilot was to generate $a_{p_x}(t)$ laterally on the control column and $a_{p_y}(t)$ on the throttle. Since for the study the problem was assumed to be on a horizontal plane, the outputs of the pilot had to be made symbolic. After necessary simple adaptation the equations for analog programming were

$$a_{e_x} = \frac{\sqrt{3}\ E_e(t_o)}{T^{1.5}} \cdot \frac{T-t}{\sqrt{1+(\frac{\hat{r}_y(t)}{\hat{r}_x(t)})^2}} \tag{3.32}$$

$$a_{e_y} = a_{e_x} \cdot \frac{\hat{r}_y(t)}{\hat{r}_x(t)} \tag{3.33}$$

a_{p_x} and a_{p_y} became pilot outputs.

$$\dot{E}_p^2 = -(a_{p_x}^2 + a_{p_y}^2) \tag{3.34}$$

$$\dot{\hat{r}}_x(t) = (a_{p_x} - a_{e_x})\ (T-t) \tag{3.35}$$

$$\dot{\hat{r}}_y(t) = (a_{p_y} - a_{e_y})\ (T-t) \tag{3.36}$$

$$\ddot{r}_x(t) = a_{p_x} - a_{e_x} \tag{3.37}$$

$$\ddot{r}_y(t) = a_{p_y} - a_{e_y} \tag{3.38}$$

$$\hat{\hat{r}}_x(t) = \hat{r}_x(t) + (a_{p_x}(t) - a_{e_k}(t))\ \frac{(T-t)^2}{2} \tag{3.39}$$

$$\hat{\hat{r}}_y(t) = \hat{r}_y(t) + (a_{p_y}(t) - a_{e_y}(t))\ \frac{(T-t)^2}{2} \tag{3.40}$$

These equations required two TR 20s again for simulation and simulation details are given in Appendix E.

As it was decided to display to the pilot the optimal trajectories along with the actual pilot feedback trajectories, the available three sets of TR 20 computers were found insufficient. It was then decided to represent the saddle point solution linearly using the analytical solutions for the differential equations (Appendix C). Using the analytical solutions for $E_p(t)$ and $r_x(t)$, the revised equation for mechanisation of the optimal trajectories became

$$a^*_{p_x} = C_1 C_2 (T-t) \tag{3.41}$$

$$a^*_{p_y} = k\, C_1 C_2 (T-t) \tag{3.42}$$

$$\dot{E}^{2*}_p = -3\, \frac{E^{2*}_p(t)}{T-t} \tag{3.43}$$

$$\dot{\hat{r}}^*_x = C_1 C_2 \left(1 - \frac{1}{C}\right) (T-t)^2 \tag{3.44}$$

$$\dot{\hat{r}}^*_y = C_1 C_2 \left(k - \frac{k}{C}\right) (T-t)^2 \tag{3.45}$$

$$\ddot{r}^*_x = \left(1 - \frac{1}{C}\right) a^*_{p_x} \tag{3.46}$$

$$\ddot{r}^*_y = \left(k - \frac{k}{C}\right) a^*_{p_x} \tag{3.47}$$

$$\hat{\hat{r}}^*_x = \hat{r}^*_x + \left(1 - \frac{1}{C}\right) a^*_{p_x} \frac{(T-t)^2}{2} \tag{3.48}$$

$$\hat{\hat{r}}^*_y = k \cdot \hat{\hat{r}}^*_x \tag{3.49}$$

where $$k = \frac{r_y(t_o)}{r_x(t_o)} \; ; \quad C = \frac{E_p(t_o)}{E_c(t_o)}$$

$$C_1 = \frac{E_p(t_o)}{T^{1.5}} \; ; \quad C_2 = \sqrt{\frac{3}{1+k^2}} \tag{3.50}$$

3.7 DESCRIPTION OF DISPLAYS

The display optimisation study was conducted by giving to the pursuer pilot in the cockpit six types of displays as described below.

3.7.1 State Vector Display

The first was a pure state vector display as indicated in Figure 3.1(a). Time to go (T-t), Energy

left $E_p^2(t)$, relative velocities in x and y directions $\dot{r}_x(t)$ and $\dot{r}_y(t)$ were displayed on voltmeters while the relative position in x and y directions r_x and r_y were displayed on an oscilloscope.

3.7.2 Quickened vector display 1

The second was one type of quickened vector display. The first order predicted misses in x and y directions were displayed on voltmeters over and above those of the first display. The relative positions of the indications are as indicated in the Figure 3.1(b). Note the close proximity of r_y, r_y and r_x, $\dot{r}_x$ for obvious reasons

3.7.3 Quickened vectors display 2

The third was again a display of first order quickened variables (Figure 3.1(c)). The only difference from the second display was that the two quantities r_x and r_y were displayed on an oscilloscope with $\dot{r}_x$ and $\dot{r}_y$ on voltmeters positioned close by as indicated in Figure This was done with the intention of providing to the pilot a visual cue, closer to the optimal control. The optimal control is given by

$$a_{p_{x(y)}}(t) = -\sqrt{\frac{3}{T-t}}\, E_{p_{x(y)}} \cdot \frac{\hat{r}_{x(y)}(t)}{\|\hat{\dot{r}}(t)\|}$$

The term $\frac{\hat{r}_x}{\|\hat{\dot{r}}\|}$ is equivalent of Cosθ in a polar representation. Display on theoscilloscope was expected to give to the human controller a direct measure of this expression, thus enabling him to do possibly better.

4.7.4 Quickened vector display 3

This is again a quickened vector display with the second order predicted miss distances displayed on the oscilloscope. Also to be displayed extra were the relative accelerations $(a_{p_x} - a_{e_x})$ and $(a_{p_y} - a_{e_y})$. The display layout is indicated in Figure 3.2(a). This quickened parameter, as would be seen, is closer to the control output of the pilot. Parameter r(t) is, as we know, is the predicted end result if the pilot were to ensure constant relative acceleration.

4.7.5 Quickened vector display 4

This display is basically the same as the previous, except that, all the corresponding parameters of the saddle point case were simultaneously presented (Figure 3.2(b)). On the oscilloscope both the actual and optimal trajectories were presented using a beam splitting device. The beam splitting was done using a function generator output to switch a relay comparator alternately, to feed the oscilloscope with the actual and optimal inputs. The operation takes place as explained in Chapter 2.

4.7.6 Control vector display

The last of the series was the control vector display. For this the optimal controls $a^*_{p_x}$ and $a^*_{p_y}$ were presented along with the instantaneous control outputs of the pilot on the oscilloscope using again the beam

splitting technique (Figure 3.2(c)). The pilot was given the 'pursuit task' of keeping his outputs aligned with those of the optimal. Unfortunately due to the system errors in the low voltage range, the outputs beyond 17 secs. out of the total 27 secs. problem time were unreliable without automatic correction for the errors. As the errors were not easily computable, such corrections could not be incorporated in the computer program. Hence the study with this display was restricted to 17 seconds.

3.8 DETAILS OF EXPERIMENTS AND DISCUSSION

3.8.1 General

The experiments were conducted for the following initial conditions.

$r_x(t_o) = 99$ ft. ; $r_t(t_o) = 2832$ ft.

$\dot{r}_x(t_o) = 0$ ft/sec ; $\dot{r}_y(t_o) = -100$ ft/sec.

$E_p^2(t_o) = 25$ ft^2/sec^3 ; $E_e^2(t_o) = 9$ ft^2/sec^3.

$T - t_o = 27$ seconds

$\hat{r}_x(t_o) = 99$ ft. ; $\hat{r}_y(t_o) = 132$ ft.

$r_x(T) = 1.8$ ft; $r_y(T) = 2.4$ ft. ; $r(T) = 3$ ft.

The runs were performed with three subjects

a) A test pilot

b) A fighter pilot with medium experience

c) An engineer with a flying background.

Before presenting each form of display the pilots were briefed about the nature of the display. In all the cases recordings were made after the subject performance had stablised with each different display. The predicted vector trajectories and state vector trajectoriss for each subject are plotted in Figures 3.3 to 3.7.

3.8.2 Experiment No.1

Parameters Displayed:

$\dot{r}_x$, $\dot{r}_y$, E_p^2, T-t on voltmeters

r_x and r_y on oscilloscope.

Observations: The performance of all the subjects was poor. While the test pilot was putting on appreciable acceleration initially the other two were not doing that even. The subjects were then told that the optimal solution needed commanding high accelerations initially, subsequentially after a number of practice runs the performance improved. The best stabilised performance of the test pilot gave r(T) = 35 feet. The performance of the other two are indicated in Table 3.2.

Subject Comments: The subjects complained that they could not judge well the effects of control on the r_x/r_y trajectory. They stated that they were giving controls in steps and waited for reaction of the state trajectory at each state. The subjects all agreed that

they tried to get the trace linearly to origin. The test pilot commented that with practice he could see that he had to maintain some relationship between the time to go (T-t) and energy left $E_p^2(t)$.

Inference: The poor performance of the subjects could be attributed to three causes:

(a) The subjects initutively tried to make the chase linear, whereas the optimal trajectory in r_x, r_y was nonlinear.

(b) The relationship between the visual cue and the control was somewhat complicated. Hence the subjects could not get a clear feedback on the effect of their control over the visual cue.

(c) The dynamic range of r_x, r_y was high. The subjects have experienced resolution problem (See Figure 3.8 for optimal trajectories).

The performance improved, as the test pilot rightly pointed out, when they learnt to see the correlation between (T-t) and $E_p^2(t)$ which is inherent in the optimal control. In other words, their performance improved when they learnt to use all the parameters required to generate the optimal control.

4.8.3 Experiment No.2

Parameters displayed:

$\hat{r}_x, \hat{r}_y, \dot{r}_x, \dot{r}_y, (T-t), E_p^2$	on voltmeters
r_x and r_y	on oscilloscope.

Observations: The performance of all the subjects improved appreciably. The best performance was that of the test pilot with r(T) = 16 ft.

Subject Comment: All the subjects expressed satisfaction.

Inference: Performance improved due to

a) The visual cue being a predicted value indicating the final outcome which is the performance index.

b) The r_x, r_y variables having a simpler relationship with pilots control a_{p_x}, a_{p_y}. Hence the subjects could sample inputs with reasonable confidence.

4.8.4 Experiment No.3

Parameter displayed: $\hat{r}_x, \hat{r}_y, \dot{r}_x, \dot{r}_y, (T-t), E_p^2$ on voltmeters

r_x, r_y, $\hat{r}_x$, $\hat{r}_y$ on oscilloscope.

Observations: During major portion of the run the performance of engineer and the second pilot came closer to optimal though towards the end it tended to become bad. The performance of the test pilot slightly deterioriated. The best final r(T) was still that of the test pilot. It was 20 ft.

Subject Comment: The test pilot felt that the resolution on the oscilloscope of r_x and r_y was bad and so he tended to look into the voltmeter values often. The other two acted in a somewhat straightforward manner of sticking to the $\hat{r}_x$, $\hat{r}_y$ oscilloscope display.

Inferences: The performance of the engineer and the second pilot is considered more meaningful as they alone have utilised the visual cue fully. As the test pilot made the observation that, he did not use the oscilloscope display of r_x and r_y, only at the end of the complete set of experiments, a rerun for him could not be conducted. Even though the resolution in the latter half of each run was not very good, it is expected that the performance of the test pilot also would have improved with this display.

This improvment at any rate of two of the subjects could be attributed to the following:

(a) The optimal trajectory in r_x, r_y was linear and this coincided with the intutive guess of the subjects. Hence their control action was directed on the right lines.

(b) The $\text{Sin}\theta(= \frac{\hat{r}_y}{\|\hat{r}\|})$ and $\text{Cos}\theta(= \frac{\hat{r}_x}{\|\hat{r}\|})$ involved in the form of the optimal control was observable in the oscilloscope display of $\hat{r}_x$ and $\hat{r}_y$.

The departure from the optimal towards the end is clearly attributable to the lack of resolution (See Figure 3.9 for optimal trajectory).

4.8.5 Experiment No.4

Parameter displayed:

$\hat{r}_x, \hat{r}_y, \dot{r}_x, \dot{r}_y, (T-t), E_p^2 (a_{p_x} - a_{e_x}), (a_{p_y} - a_{e_y})$ in voltmeter

$r_x, r_y, \hat{\hat{r}}_x, \hat{\hat{r}}_y$ in oscilloscope.

Observations: The r_x, r_y and $\hat{r}_x$, $\hat{r}_y$ trajectories for all kept quite close to the optimal in the major portion of the run. However, the system due to characteristics got always overloaded toward the end forcing the run to be stopped. There was fair amount of hunting in the trace in the second half of all the runs.

Subject comment: All the subjects expressed satisfactions with the display in that the response of the trace to the control was instantaneous and appreciable. However, the movement of the trace was too fast. This combined with low values of r_x and r_y for considerable portion of the problem, made them not exercise steady control in the end (See Figure 3.10) for optimum trajectories).

Inferences: The reason in the improvement in the first half was directly due to visible correspondence of the trace with the control. The deterioration towards the end could be attributed to two reasons.

(a) For more than half the time the voltage levels of r_x, r_y were low. The circuit for generation of these two quantities use a maximum number of seven nonlinear elements. The nominal error in each multiplier is 40 mV. The cumulative error due to the nonlinear elements decidedly becomes comparable to the parametric voltage level. This caused repeated overloading of the system.

(b) In the zone where the voltage levels were low, the errors in the control outp ut of the pilot, became rather high comparitively. This leads to the overloading of the system.

A true comparison between the relative merit of $\hat{r}(t)$ and $\hat{\hat{r}}(t)$ as display parameters could not be made. A more accurate computational facility like that of using a digital computer instead of the analog, would have enabled the experimenter to avoid the system error and ascertain the true value of $\hat{r}(t)$ display. Though it is reasonable to expect $\hat{\hat{r}}(t)$ to give better results, this could not be conclusively proved.

4.8.6 Experiment No.5

Parameters displayed: All parameters of last experiment, along with their optimal counter parts.

Observations: Performance by all the subjects did not alter much.

Subject Opinion: All the subjects stated that intuitively they had been attempting the same trajectories even in the last experiment.

Inferences: It so happens that the optimal trajectories for $\hat{r}$ and $\hat{\hat{r}}$ in this problem were linear. Had the optimal trajectories been nonlinear or even only piecewise linear it stands to reason that performance would have improved with the simultaneous display of the optimal.

4.8.7 Experiment No.6

Parameters displayed: a_{p_x}, a_{p_y}, $a^*_{p_x}$, $a^*_{p_y}$

Observations: The performance of the test pilot was the best with only a 9 feet error from that of the optimal at the

end of 17 seconds while that of the second pilot registered about 20 feet.

Subject Opinion: The task for 17 seconds was found to be simple by all.

Inference: The pilot task was a simple pursuit. Hence the performance in the reliable system operation zone was found the best. However, it took away from the pilot the capability to apply corrections for the system errors since he did not have a measure of the end result displayed to him in the case of the predicted miss distance displays.

3.9 CONCLUSION

Predicted displays indicating the end results all the time are distinctly superior to state vector displays for terminal range fixed time problems. This qualitative results agrees with that of Baron[12] and that of Warner[13]. Extensions of Baron's result were attempted in the experiments numbers 3,4 and 6. It was seen that providing predicted displays of a higher order with more direct correlation with pilots control may improve the performance. But this could not conclusively be proved due to system shortcomings. The control vector display was found indeed the best provided the control computation could be accurate. If control computation becomes inaccurate, this display will result in drastic deterioration in results.

The performance of the test pilot was found to be the best on the average. This could be expected. The performance of the engineer with a general flying background was found better on the average than the fighter pilot with medium experience. The test conditions in this simulator study were of course not that exacting as that of an actual combat mission in which case the pilot with his flying experience would have been assuredly the better of the two. All the same, it would appear correct to conclude that an engineer pilot would be capable of providing meaningful results in qualitative studies. His adaptability to flight simulator and its varying displays was comparable to that of a test pilot and better than an average fighter pilot.

Table 3.2

PERFORMANCE TABLE

Display	Test pilot	Best Average Performance r(T)	
		Average pilot	Engineer
1	35 ft.	80 ft.	50 ft.
2	16 ft.	33 ft.	27 ft.
3	20 ft.	26 ft.	26 ft.
4	-	-	-
5	-	-	-
6	9 ft.	20 ft.	Could not be recorded but observed to be close to that of the average pilot

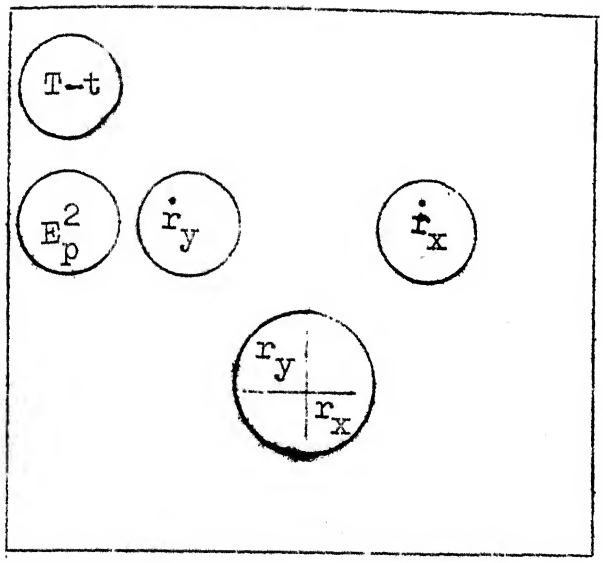

(a)

(b)

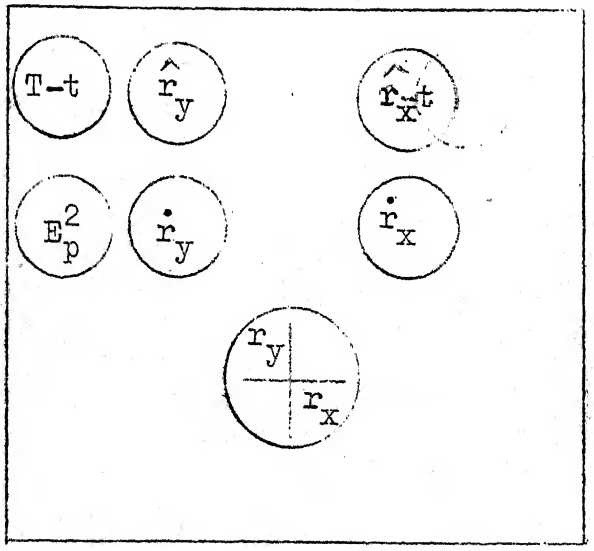

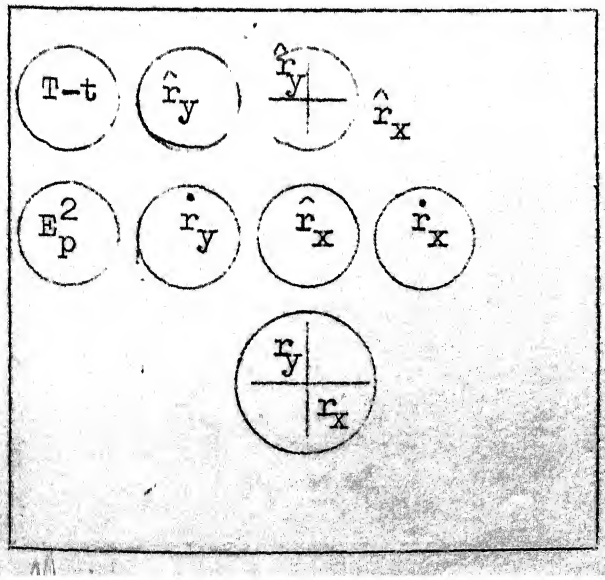

(c)

FIG. 3.1 DISPLAY VARIATIONS I

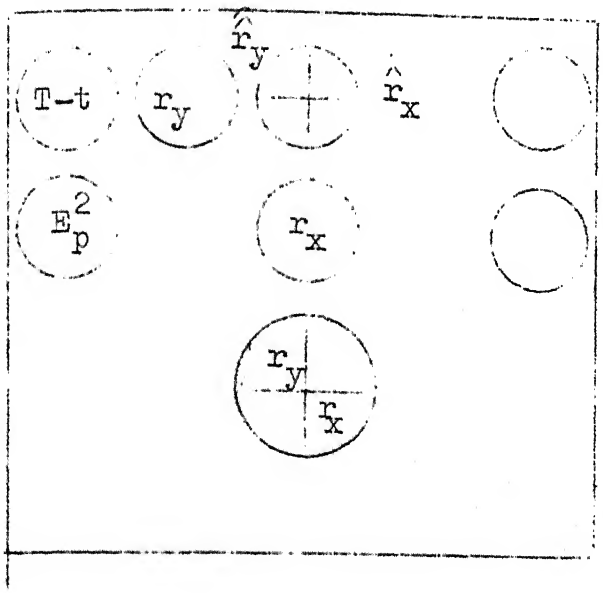

(a)

(b)

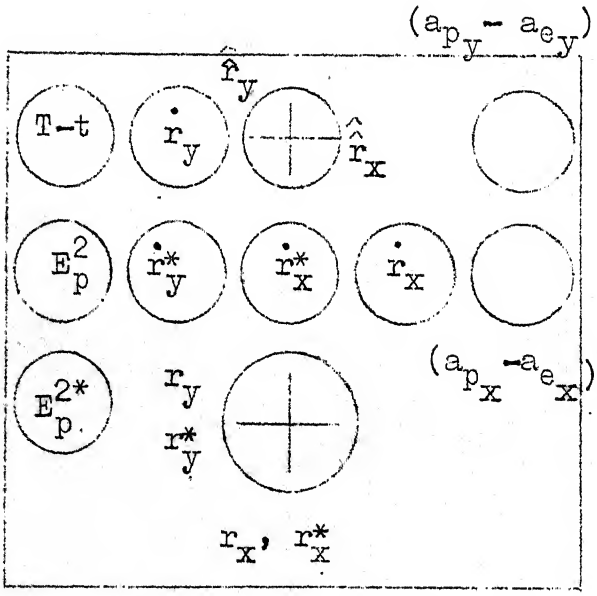

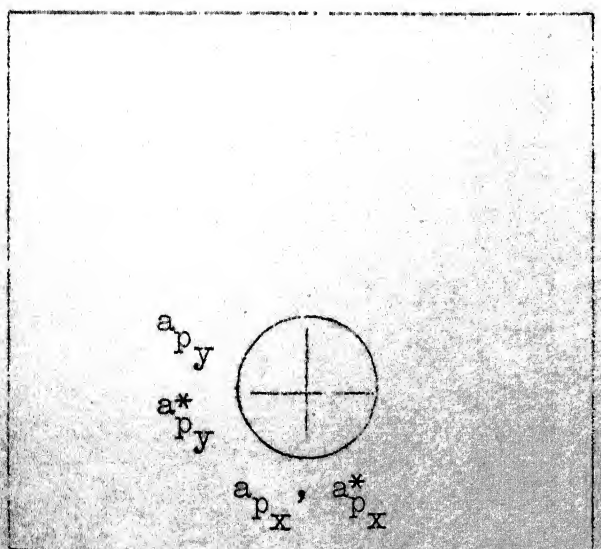

(c)

FIG.3.2: DISPLAY VARIATIONS II

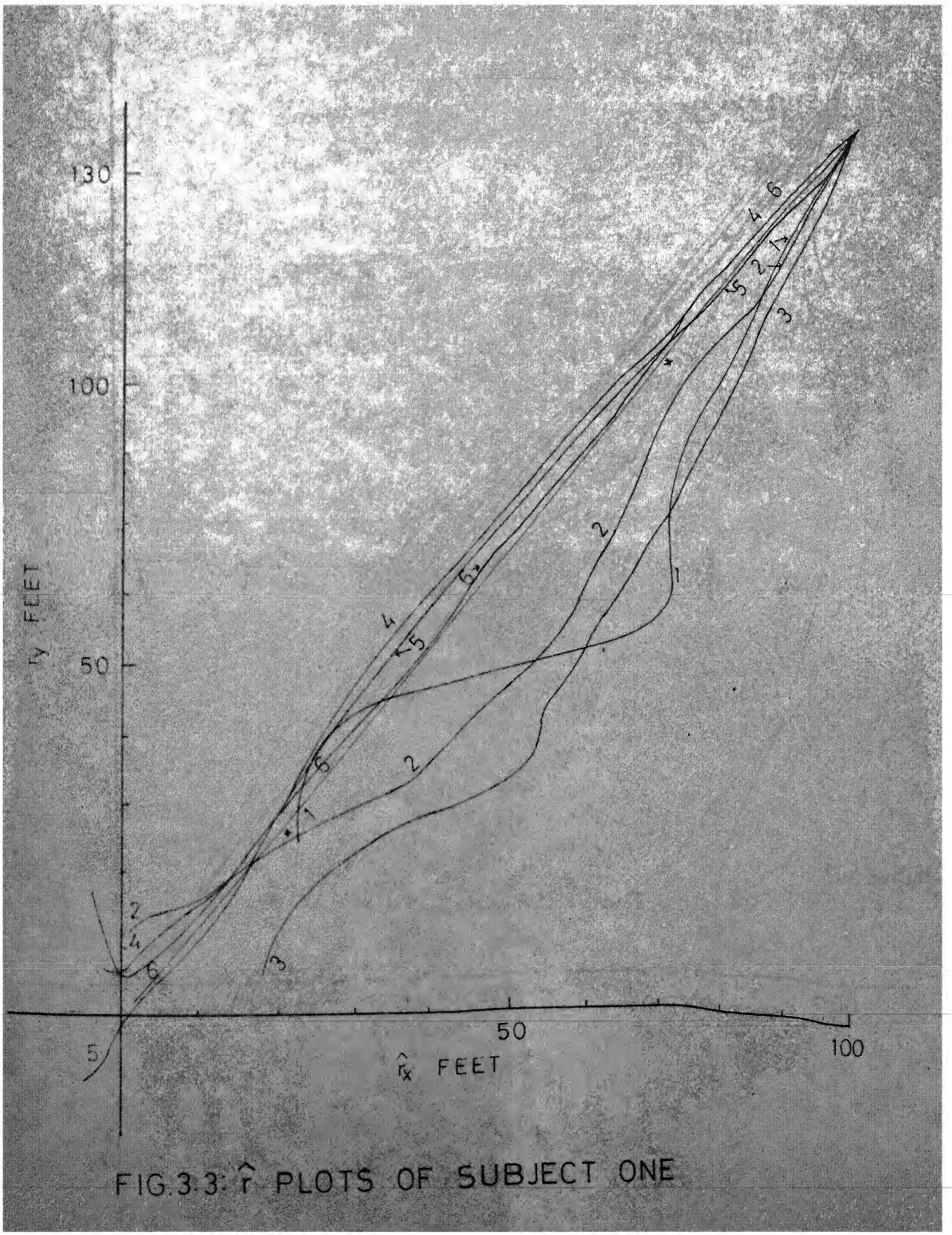

FIG. 3.3: $\hat{r}$ PLOTS OF SUBJECT ONE

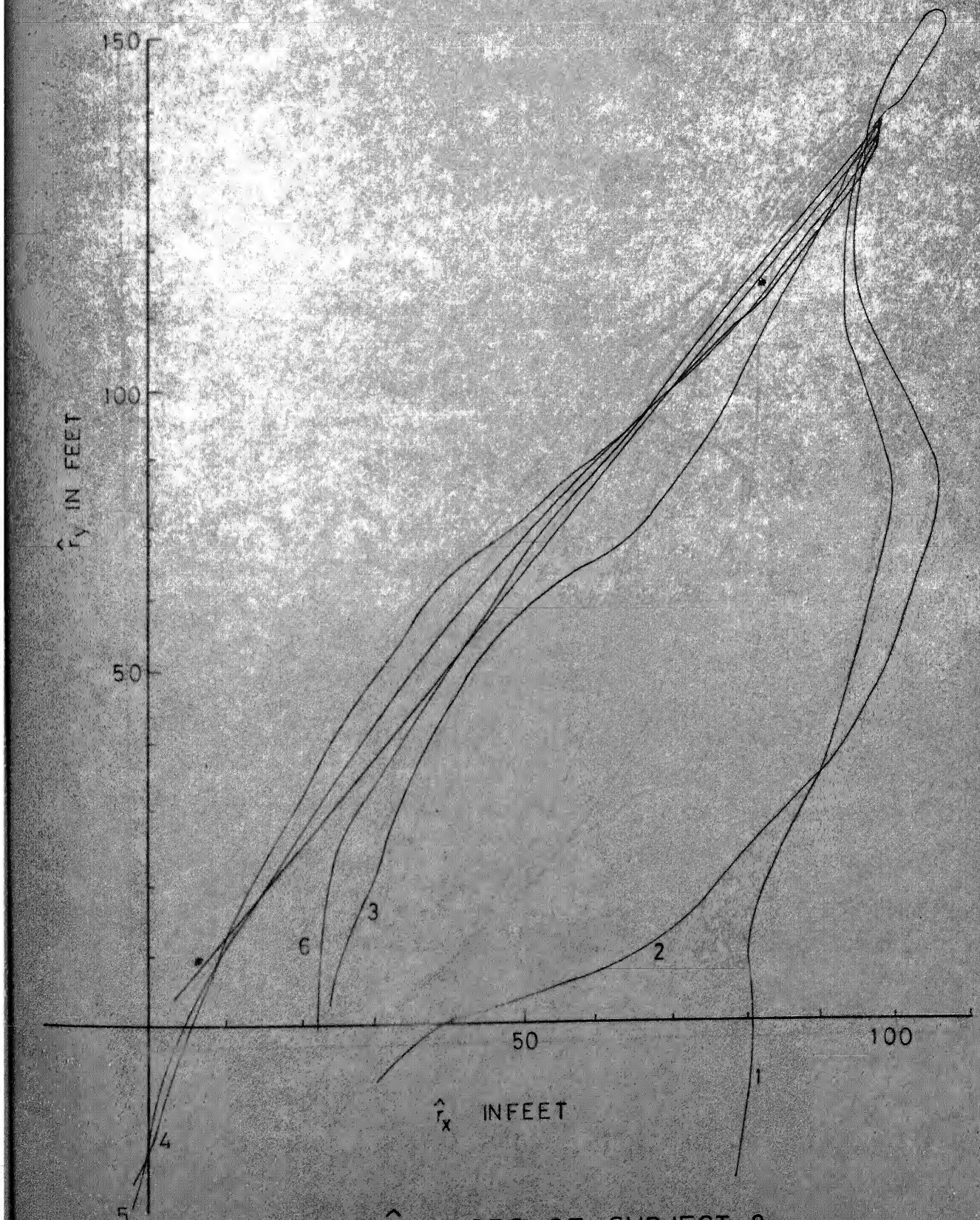

FIG.3.4: $\hat{r}$ PLOTS OF SUBJECT 2

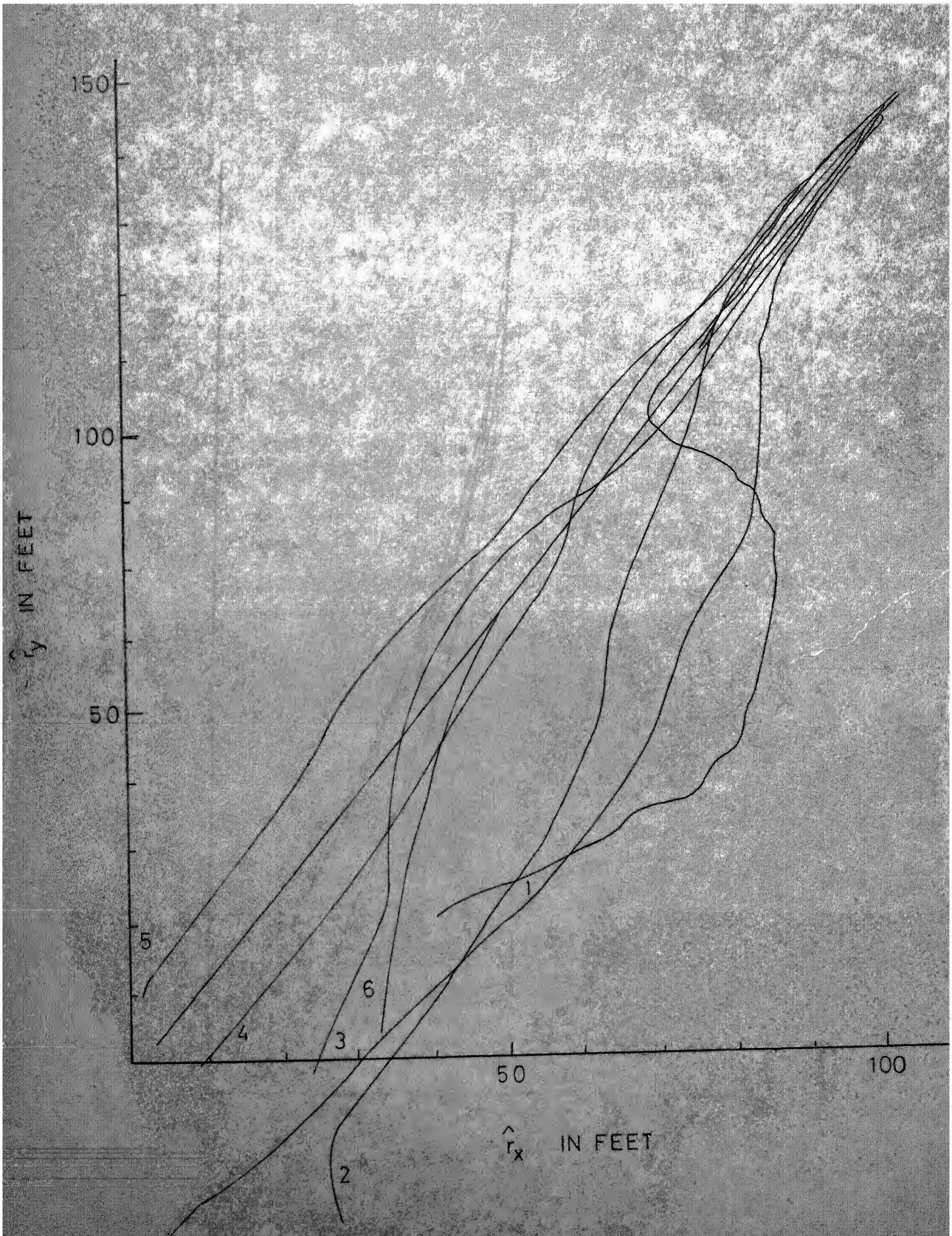

FIG. 3.5: $\hat{r}$ PLOTS OF SUBJECT 3

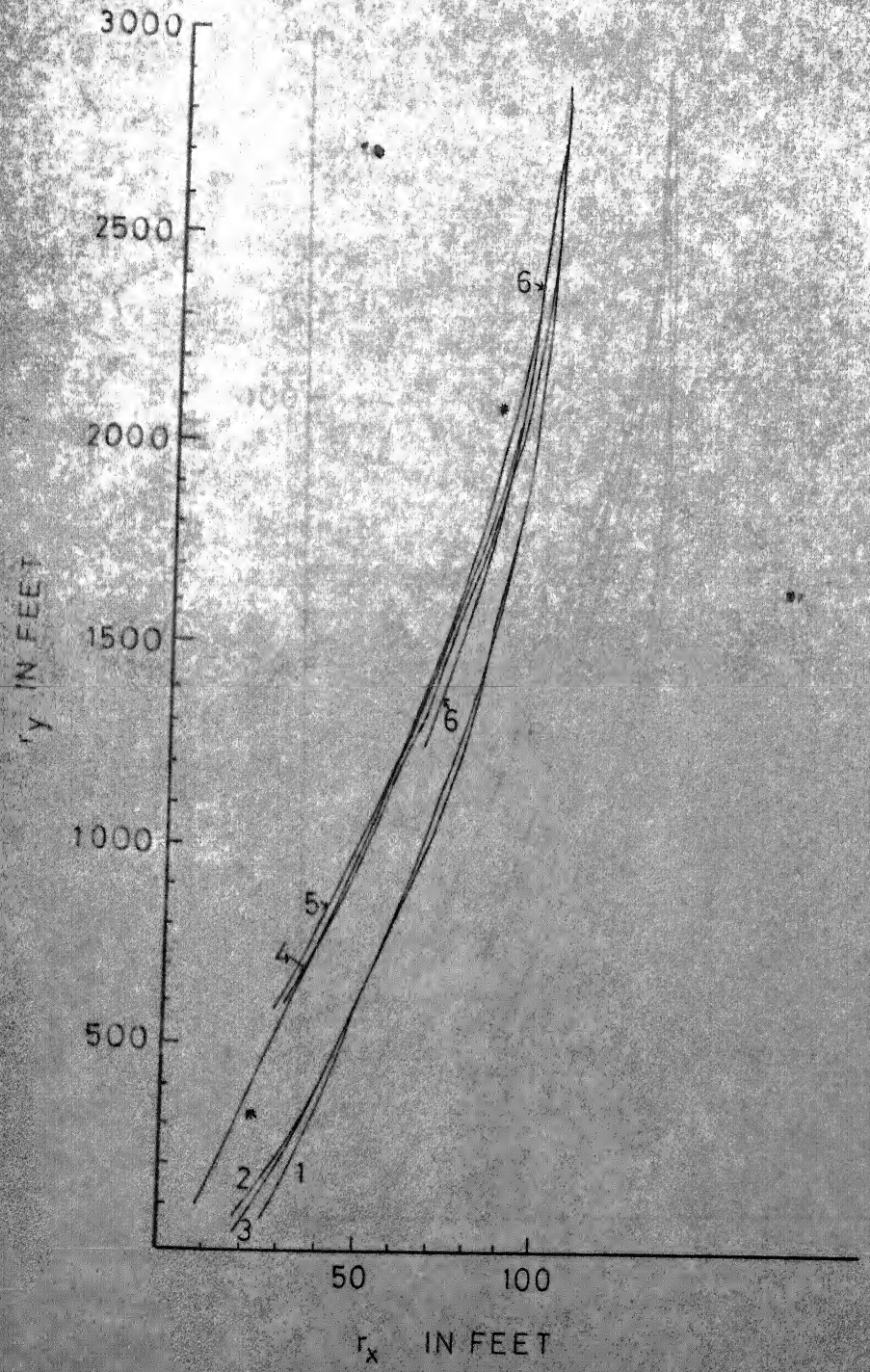

FIG. 3.6: r PLOTS OF SUBJECT ONE

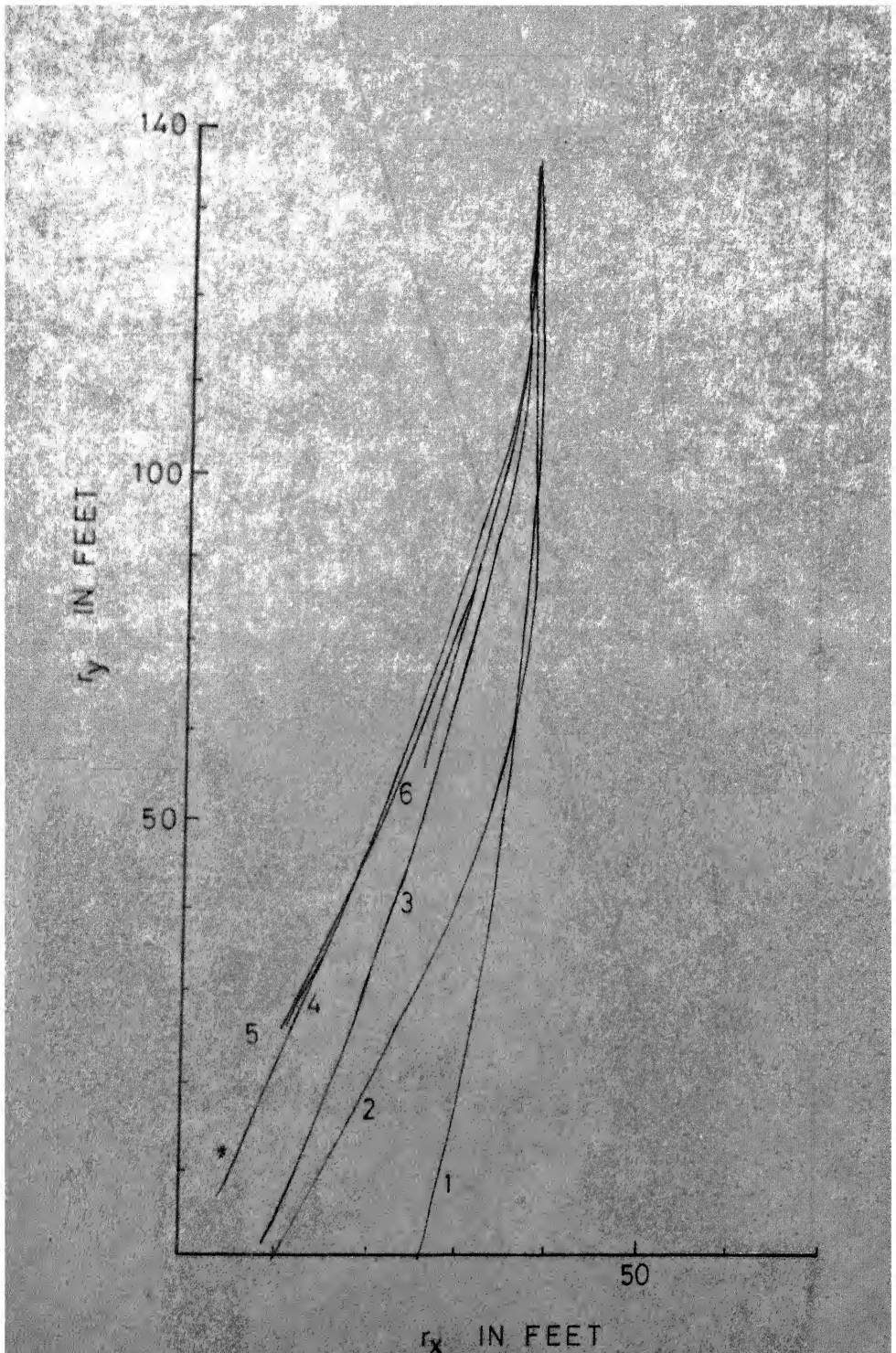

FIG.3·7: r PLOTS OF SUBJECT 2

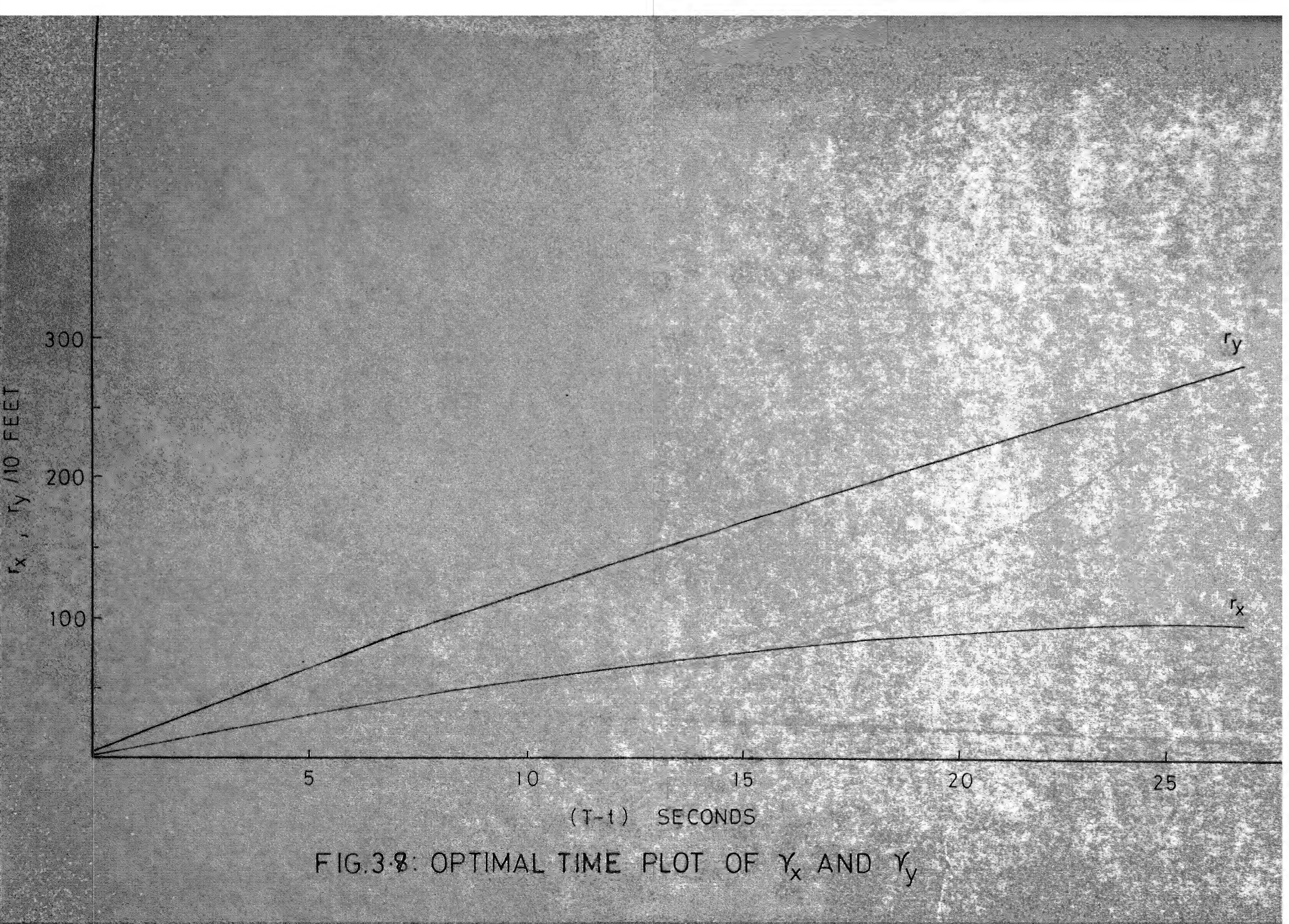

FIG. 3.8: OPTIMAL TIME PLOT OF γ_x AND γ_y

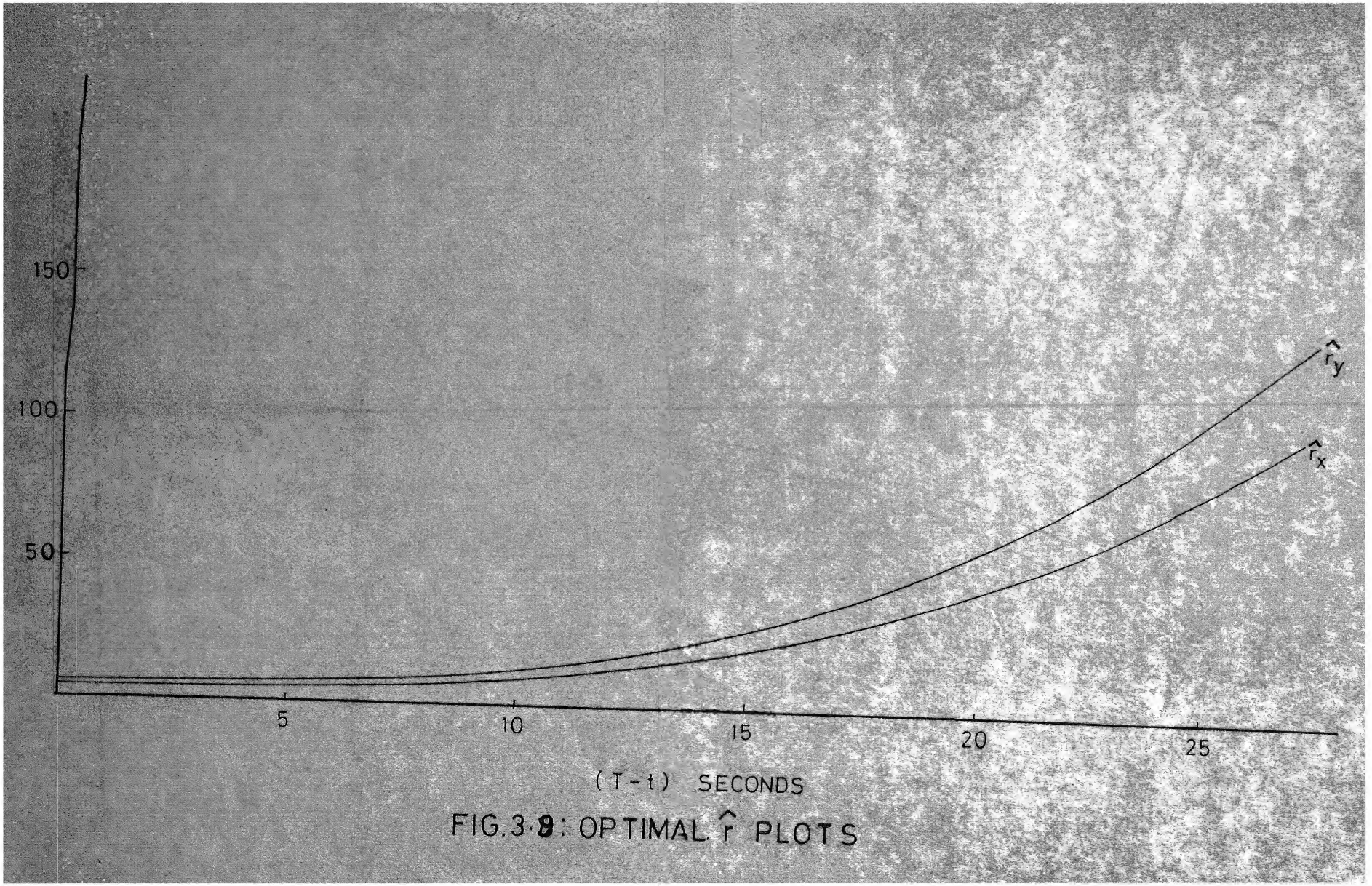

FIG. 3.8: OPTIMAL $\hat{r}$ PLOTS

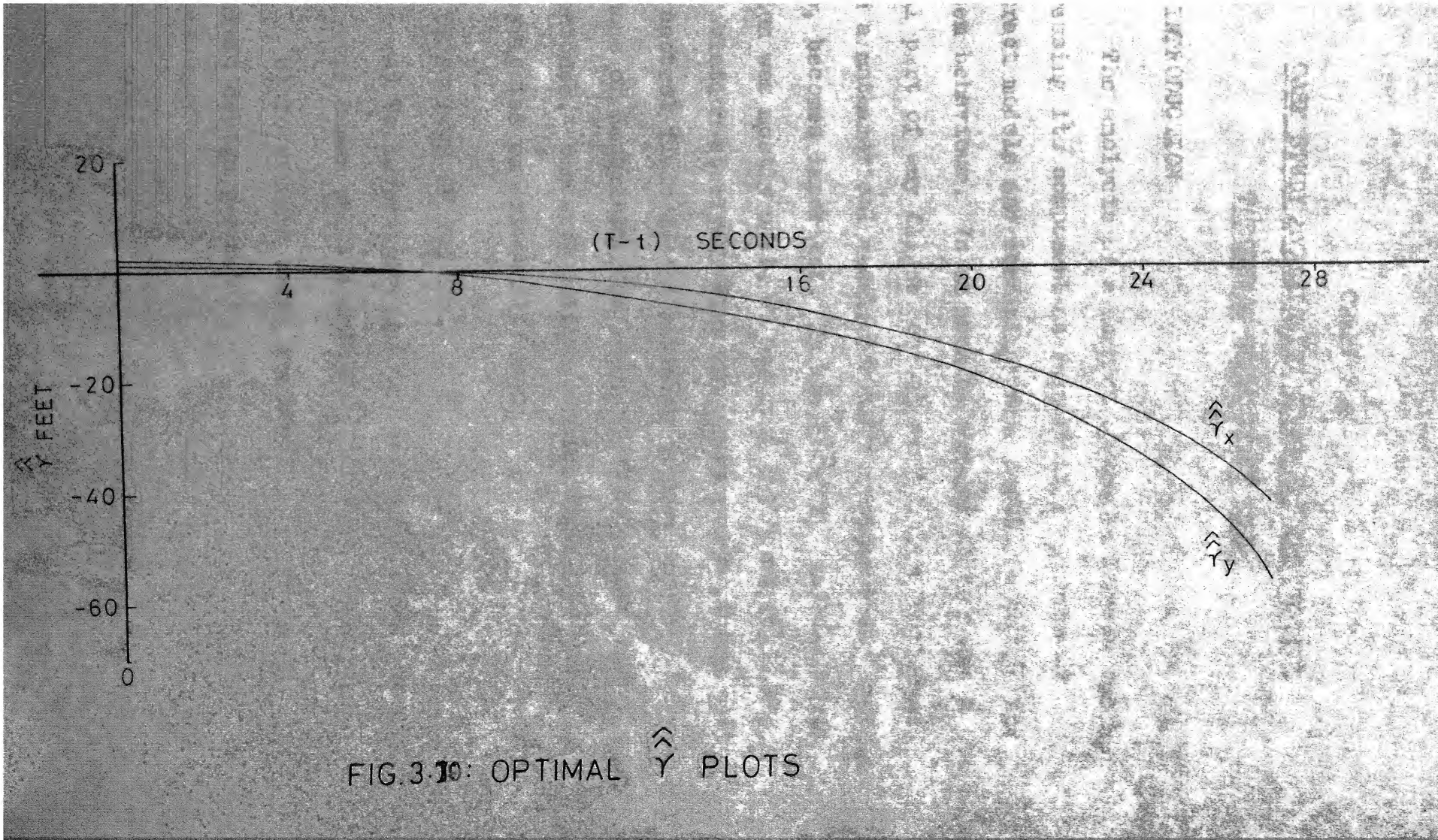

FIG. 3.10: OPTIMAL $\hat{\hat{Y}}$ PLOTS

CHAPTER 4

CASE STUDY 2:VALIDATION OF AN OPTIMAL CONTROL THEORETIC HUMAN PILOT MODEL

4.1 INTRODUCTION

The analysis of a control system is carried out by expressing its component characteristics in terms of abstract models and combining these models to obtain the system behaviour. In as much as a human pilot forms a vital part of any flight control system, development of such a mathematical model, for human responses in a closed loop, becomes important. In the fifties, quasilinearisation was mostly used, to develop the human pilot model for aviation studies. With the rapid growth of the optimal control field in the sixties, optimal control theoretic methods of describing the human pilot response have gained importance. One such optimal control theoretic model is investigated experimentally here.

4.2 OBJECTIVES OF THE STUDY

a) To investigate and identify an optimal control theoretic human pilot model in a tracking situation.

b) To attempt using the model in choosing an aircraft design parameter.

4.3 MODEL DESCRIPTION[14]

The model developed by Blank and Schumacher[14] is based on the stipulation that the performance of a human operator in a tracking situation corresponds to that of an optimal controller which minimizes a quadratic cost functional. If this theory were to be true, the dynamics of the theoretically derived optimum controller should match those of the human operator. The plant is described by the state equation

$$\dot{\underline{x}} = \underline{A}\,\underline{x} + \underline{B}\,\underline{u} \tag{4.1}$$

The tracking system is described by

$$\dot{\underline{z}} = \underline{D}\,\underline{z} \tag{4.2}$$

Cost functional to be minimised is

$$J = \tfrac{1}{2}\,\underline{e}^{T}(T)\underline{F}\,\underline{e}(T) + \tfrac{1}{2}\int(\underline{e}^{T}\,\underline{Q}\,\underline{e} + \underline{u}^{T}\,\underline{R}\,\underline{u})\,dt \tag{4.3}$$

where

$$\underline{e} = \underline{z} - \underline{y}$$

This tracking problem is then reduced to an equivalent regulator problem.

An observation vector $\underline{y}_a$ is constructed as

$$\underline{y}_a = \underline{C}_a\,\underline{x}_a$$
$$x_a = \begin{bmatrix} z \\ \cdots \\ \underline{x} \end{bmatrix} \tag{4.4}$$

The overall system can be written similarly

$$\begin{bmatrix} \dot{z} \\ \cdots \\ \dot{x} \end{bmatrix} = \begin{bmatrix} D & \vdots & 0 \\ \cdots & & \cdots \\ 0 & \vdots & A \end{bmatrix} \begin{bmatrix} z \\ \cdots \\ x \end{bmatrix} + \begin{bmatrix} B_1 \\ \cdots \\ B_2 \end{bmatrix} u \qquad (4.5)$$

or

$$\dot{x}_a = A_1 x_a + B u \qquad (4.6)$$

where

$$B = \begin{bmatrix} B_1 \\ \cdots \\ B_2 \end{bmatrix} = \begin{bmatrix} 0 \\ 0 \\ \cdots \\ 0 \\ 1 \end{bmatrix}$$

Defining

$$C_a = \begin{bmatrix} 1 & 0 & -1 & 0 \\ 0 & 1 & 0 & -1 \end{bmatrix} \qquad (4.7)$$

$$y_a = C_a x_a$$

enables the difference between z and x to appear explicitly as observations. Now cost functional

$$J = \tfrac{1}{2}\int_0^T (y_a^T Q y_a + u^T R u)\, dt$$

where

$$Q = \begin{bmatrix} q_{11} & 0 \\ 0 & q_{22} \end{bmatrix} \qquad (4.8)$$

and $R = [r]$

By a judicious selection of Q and R the system response can be controlled.

Recognising this a standard linear regular problem, we can write,

$$u^* = -\underline{R}^{-1}\ \underline{B}^T\ \underline{R}\ \underline{k}\ \underline{x}_a \qquad (4.9)$$

where $\underline{k}$ is the 4x4 symmetric time varying matrix solution of the matrix Riccati equation

$$-\dot{\underline{k}} = \underline{k}\ \underline{A}_1 + \underline{A}_1^T\ \underline{k} - \underline{k}\ \underline{B}\ \underline{R}^{-1}\ \underline{B}^T k + \underline{C}^T \underline{Q}\ \underline{C} \qquad (4.10)$$

Blank and Schumacher consider[14] a parallel infinite time problem with transfer function of the controlled element assumed as $\frac{k_c}{s(s+a)}$ and the system taken to be of a single input single output type.

The optimal control representation is converted[14] to that of a transfer function type to yield the following system transfer function and pilot transfer function.

$$\frac{x}{z}(s) = \frac{\frac{\hat{k}_{24}}{r}(s+\frac{\hat{k}_{14}}{\hat{k}_{24}})}{s^2+(a+\frac{\hat{k}_{44}}{r})s+\frac{\hat{k}_{34}}{r}} \qquad (4.11)$$

$$\frac{u(s)}{E(s)}\left(\ G(s)\ \right) = \frac{\frac{\hat{k}_{24}}{r}(s+\frac{\hat{k}_{14}}{\hat{k}_{24}})s(s+a)}{s^2+s(a+\frac{\hat{k}_{44}}{r}-\frac{\hat{k}_{24}}{r})+\frac{\hat{k}_{34}}{r}-\frac{\hat{k}_{14}}{r}} \qquad (4.12)$$

The block diagram representation would be as in Figure 4.1.

4.4 MODEL INVESTIGATION PROCEDURE

The following were the steps involved in the experimental study.

a) Assume some form of tracking model and plant model, and programme the system on the analog computer.

b) Choose a good representative set of values for q_{11}, q_{22} and r. Solve the Riccati equation and obtain k_{i4} (i=1,4) values.

c) Incorporate the model of the pilot corresponding to each set of q_{11}, q_{22} and r on to the analog set up. Run the computer till steady state is reached and record the trajectories for u*, e and de/dt where e is the error z-x.

d) Put an experienced pilot in place of the optimal controller. Display the system controller inputs on the flight simulator display panel, plot the u_{pilot}, e and de/dt while the pilot is controlling the system.

e) Compare the trajectories generated by the pilot with those of the models. Check, for behaviour similarity and see whether any particular optimal model checks well with the pilot's. This validates/invalidates the model and helps in identifying the weightages q_{11}, q_{22} used by the pilot.

f) Vary the aircraft parameter which is be decided upon, and in each case evaluate on the computer, the value

of the performance index $= \int_0^T \{(q_{11}e^2(t) + q_{22}e^2(t) + ru^2(t)\} dt$

See whether the variation in J gives any indication as to the choice of the aircraft parameter.

4.5 EXPERIMENTAL DETAILS FOR MODEL VALIDATION AND DISCUSSION

4.5.1 Simulated Optimal Closed Loop System

The tracking model chosen is described by

$$\ddot{z} + 0.1\,\dot{z} + 0.01\,z = 0$$
$$z(o) = 7.5\ ;\quad \dot{z}(o) = 0 \qquad (4.13)$$

The controlled element chosen was

$$\ddot{x} + 2\dot{x} = u(t)$$
$$x(o) = 7.5\ ;\quad \dot{x}(o) = 0 \qquad (4.14)$$

The plant was representative of the attitude control of a jet aircraft in hover. The block diagram of the closed loop system with the optimal controller would then be as indicated in Figure 4.1. As a representative set of weightages for e and $\dot{e}$, possibly used by pilot, q_{11} and q_{22} were chosen as various combinations 1, 10, 100. For various combinations possible in q_{11} and q_{22}, values for r of 1, 0.1 and 0.01 were chosen. The solution for 'k' obtained, integrating the Riccati equation backwards in time for all possible combinations of the above values for q_{11}, q_{22} and r are presented in Table 4.1. Corresponding to each set of values, different optimal control models emerge. These, taken

one at a time, along with the tracked model and the plant model, form the feedback loop to be simulated. In all the above cases it was seen that

$$\frac{\hat{k}_{14}}{r} = \frac{\hat{k}_{34}}{r} \quad \text{and} \quad \left(a + \frac{\hat{k}_{44}}{r} - \frac{\hat{k}_{24}}{r}\right) \quad 0 \qquad (4.15)$$

The Transfer function (4.12) then reduces to

$$G(s) = \frac{\frac{\hat{k}_{24}}{r}\left(s + \frac{\hat{k}_{14}}{\hat{k}_{24}}\right)(s+a)}{s} \qquad (4.16)$$

The above system was programmed in the analog computer (Appendix F). The computer runs were performed for each of the twenty seven models in Table 4.1 and the u*, e and de/dt, the components of J, were plotted against time. The plots indicated that by 80 seconds steady state values were reached. Hence T = 80 seconds was chosen as problem evaluation time in the study.

4.5.2 Simulation with Human Pilot in the Closed Loop

An experienced Air Force pilot was used as the subject in the piloted runs. The error e = z-x was displayed with a good sensitivity of 0.1 volt per cm on the oscilloscope in the display unit. The pilot replaced the optimal theoretic controller in the flight simulator system (refer Figure 4.2). To avoid effects of external audiovisual disturbances on the pilot, the simulator

cockpit was enclosed by wooden curtains and silence was observed in the area except for the sound of the recorder operation. The pilot then was given the compensatory task of keeping the error zero during the simulator run. The pilot was given repeated runs on the flight simulation facility till his performance stablised.

4.5.3 Pilot Model Identification

The pilot exhibited quick learning behaviour. His performance stabilized after 5 consecutive runs of each 80 seconds duration. The stabilized record for [illegible] u,e and de/dt are shown in Figures 4.3, 4.4 and 4.5. The 'u' plots recorded for the human pilot were compared with u* plots taken earlier. The pilot's plots, in general, showed good similarity with the optimal control plots. In particular the plot for $q_{11} = 100$, $q_{22} = 100$, $r = 1.0$ appeared almost identical with the averaged u plot of the pilot (Figure 4.3). A comparison of the respection plots for error e in the piloted run and the optimal control run for the weightages of (100, 100, 1), indicated an average error of less than ± 0.04 volts. The piloted plot for de/dt was oscillating uniformly over the zero line indicating an average of 0.0 similar to the optimal model second. Thus it appeared that for plant damping ratio of 2, the pilot behaved in a manner almost identical to an optimal control model minimizing a performance index given in next page.

$$J = \frac{1}{2}\int_0^T (100\, e^2(t) + 100\dot{e}^2(t) + u(t))dt \qquad (4.17)$$

With these weightages, the computer was programmed for measurement of the performance index values for optimal controller and the subject pilot. The measured values for the two were very nearly the same.

For this set of values,

$$G(s) = \frac{11.0(s+0.9)(s+2)}{s} \qquad (4.18)$$

4.5.4 Model Varification

As a further verification on the model obtained, it was decided to compare this with the quasilinear model obtained by Mcruer and Krendal in a compensatory task with random input signal. For a signal bandwidth of 1 rad./second the $G(s)$ was found as

$$G(s) = \frac{100e^{-0.15s}(2s+1)}{(0.25s+1)(0.67s+1)} \qquad (4.19)$$

An approximation to the above in consideration of natural frequency of 0.1 rad./sec. in the system input yields

$$G(s) = \frac{8(s+0.5)}{s} \qquad (4.20)$$

The similarity between (4.18) and (4.20) is noticeable. The zero at -2 in (4.18) could be attributed to the fact that the input was deterministic in our case. The optimal controller (operator) was able to learn the task and effectively cancel the pole of the plant at -2.

The other zero at 0.9 is comparable with that of -0.5 of Mcruer's model. This zero is representative of the $1/T_L$ term with T_L the lead coefficient. Due to the deterministic nature of the input, the optimal controller (operator) needed to generate only a lesser lead term of 1/0.9 as against the 1/0.5 that was generated with a random input.

4.6 USE OF MODEL FOR PARAMETER CHOICE

4.6.1 Choice of Parameter

The plant (VTOL aircraft in hover) transfer function used was $k_c/(s(s+a))$ where 'a' was the pitch damping ratio of the aircraft. It was decided to use the quadratic performance index of the operator with the identified weightages to choose the pitch damping ratio.

4.6.2 Experimental Details and Discussion

Piloted runs of the simulator were given for different values of the plant damping ratio ranging from 0 to 3.0. The performance was computed in each case over the usual period of 80 seconds. The performance index 'J' was then plotted against the plant damping ratio 'a' (Figure 4.6). The plot indicates that the value of J is uniformly minimum for a damping range of 0 to 1 and is low enough till a value of 1.5 for a.

As a parallel criterion, the pilots verbal ratings were asked. The experienced pilot, however, indicated that he could not give any distinct comparative ratings. It was felt that for the pilot used who had a vast flying experience of over 15000 hours, the single axis task with a deterministic input would have been too simple for a comparative study. As a follow up, an engineer with an elementary flying background was tried out. The performance index values were naturally higher than the pilot's but indicated a minimum between 0.5 to 1 damping and reasonably low between 0.25 to 1.5. Asked to comment, the engineer pilot expressed a clear choice for the plant configuration with damping ratio between 0.5 to 1.5.

The above results were compared with those of Lollar obtained experimentally for a random input. The value for damping ratio of 0.75 was recommended by Lollar. This we see lies in the range for 'a' arrived at in our study. Thus J was useful for indicating approximately the range for choice of the design parameter. Further, the pattern in variation of J with plant damping leads us to suspect that under more realistic condition of random inputs even the experienced pilot would have felt the difference in performance due to damping ratios in which case the performance index J could serve as an aircraft rating index.

As a matter of further interest, it was decided to compare the optimal controller performance with that of the experienced pilot for the various values of plant damping. For this the Riccati equation was solved on digital computer for varying values for 'a' (Table 4.2). The optimal controller arrived at, was incorporated on the analog computer and the values for performance index, were computed. These were plotted against 'a' (Figure 4.6). The plot was found remarkably close to that of the experienced pilot. This does indeed provide greater confidence in the validity of the premise that a human operator, in the tracking situation considered, performs like an optimal controller.

4.7 CONCLUSION

In the case study, an optical control theoretic model for human pilot was described. The model was applicable for a tracking task with deterministic input and plant description of $k_c/(s(s+a))$. By experimental studies using an experienced pilot, it was seen that the model with weightages 100, 100, 1 for error, error rate and control in the quadratic cost function does satisfactorily represent the human pilot response under the conditions mentioned. This model was also found satisfactory with varying plant damping ratios and conforms to the quasi-linear model of Meruer. The study in no way proved the model to be the unique one for representation of human pilot responses. However, it does assure us that the

model developed from optimal control theoretic considerations, can indeed be used as a valid representation in basic design of aircraft.

The study also indicated that the unified performance index of the optimal control model can serve to identify reasonable zones for locating aircraft design parameter. Its equivalence to pilot ratings as an aircraft classification index could not, however, be fully substantiated from the subject pilot opinion. However, from a study of the pattern of variation of J, it may not be unreasonable to expect that with random inputs given, the subject pilot ratings would have shown variations. The performance index may then have been found to serve effectively as an aircraft rating index.

Table 4.1

STEADY STATE VALUES FOR $\hat{k}_{ij}$ for a = 2

#	q_{11}	q_{22}	r	$\hat{k}_{14}$	$\hat{k}_{24}$	$\hat{k}_{34}$	$\hat{k}_{44}$
1	1	1	1	0.96	2.16	1.00	0.65
2	1	1	0.1	0.31	0.43	0.32	0.25
3	1	1	0.01	0.10	0.11	0.10	0.09
4	1	10	1.0	0.96	3.54	1.00	2.00
5	1	10	0.1	0.31	1.03	0.32	0.85
6	1	10	0.01	0.10	0.32	0.10	0.30
7	1	100	1.0	0.96	9.93	0.99	8.30
8	1	100	0.1	0.31	3.16	0.32	2.98
9	1	100	0.01	0.10	0.98	0.10	0.96
10	10	1	1.0	3.14	3.14	3.16	1.36
11	10	1	0.1	1.00	0.57	1.00	0.38
12	10	1	0.01	0.32	0.13	0.32	0.11
13	10	10	1.00	3.14	4.28	3.16	2.51
14	10	10	0.1	1.00	1.10	1.00	0.91
15	10	10	0.01	0.32	0.33	0.32	0.31
16	10	100	1.00	3.14	10.29	3.16	8.50
17	10	100	0.1	0.99	3.19	1.00	3.00
18	10	100	0.01	0.31	0.98	0.31	0.96
19	100	1	1.0	9.99	4.86	10.00	3.00
20	100	1	0.1	3.16	0.87	3.16	0.68
21	100	1	0.01	1.00	0.17	1.00	0.15
22	100	10	1.00	9.99	5.69	10.00	3.83
23	100	10	0.1	3.16	1.28	3.16	1.09
24	100	10	0.01	1.00	0.35	1.00	0.33
25	100	100	1.00	9.99	11.0	10.00	9.14
26	100	100	0.1	3.16	3.26	3.16	3.07
27	100	100	0.01	0.98	0.99	0.98	0.97

Table 4.2

$\hat{K}_{ij}$ for various 'a's

a	$\hat{k}_{14}$	$\hat{k}_{24}$	$\hat{k}_{34}$	$\hat{k}_{44}$
0.0	9.99	10.854	10.00	10.954
0.25	9.989	10.856	10.00	10.707
0.5	9.99	10.863	10.00	10.466
0.75	9.989	10.874	10.00	10.230
1.00	9.989	10.890	10.00	10.000
1.5	9.988	10.934	10.00	9.557
2.0	9.986	10.995	10.00	9.136
2.5	9.984	11.074	10.00	8.736
3.0	9.982	11.168	10.00	8.358

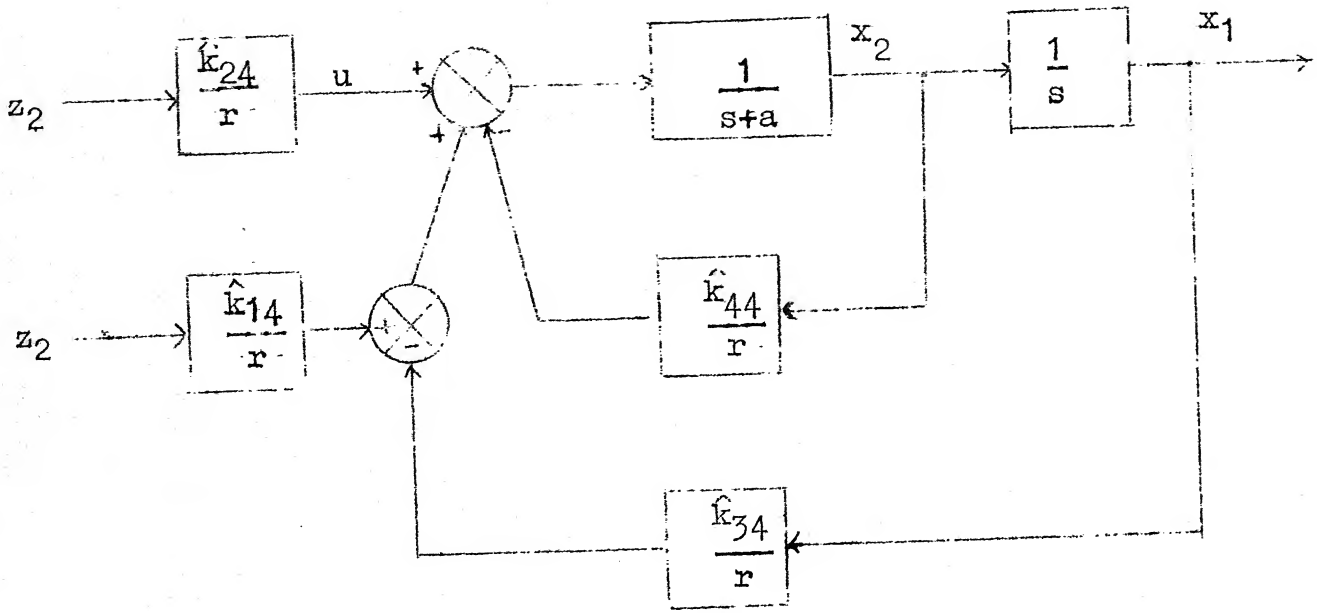

FIG.4.1 OPTIMAL CONTROLLER LOOP

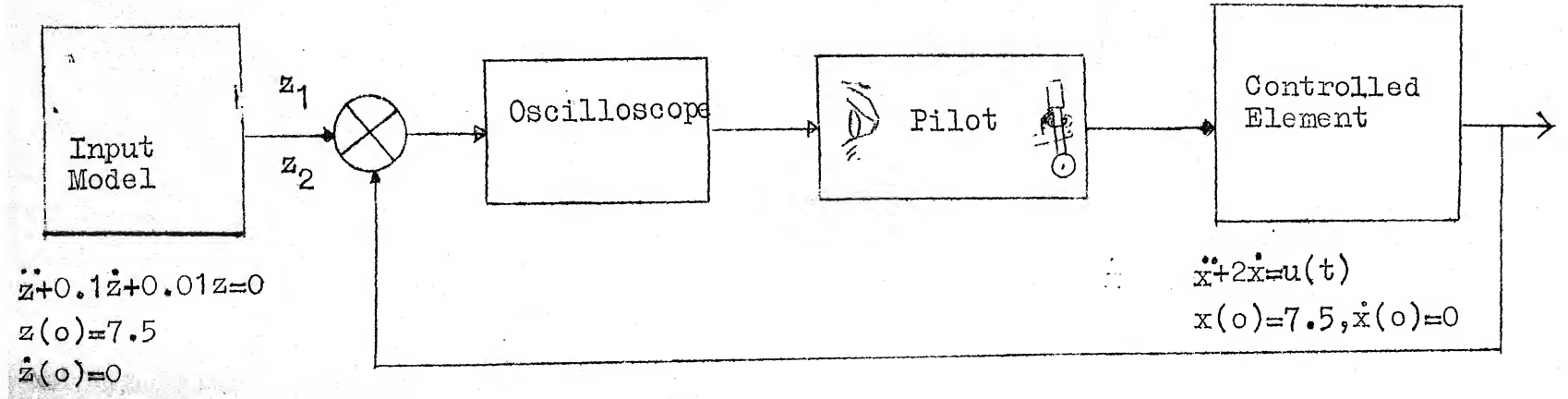

FIG.4.2 PILOTED FEEDBACK LOOP

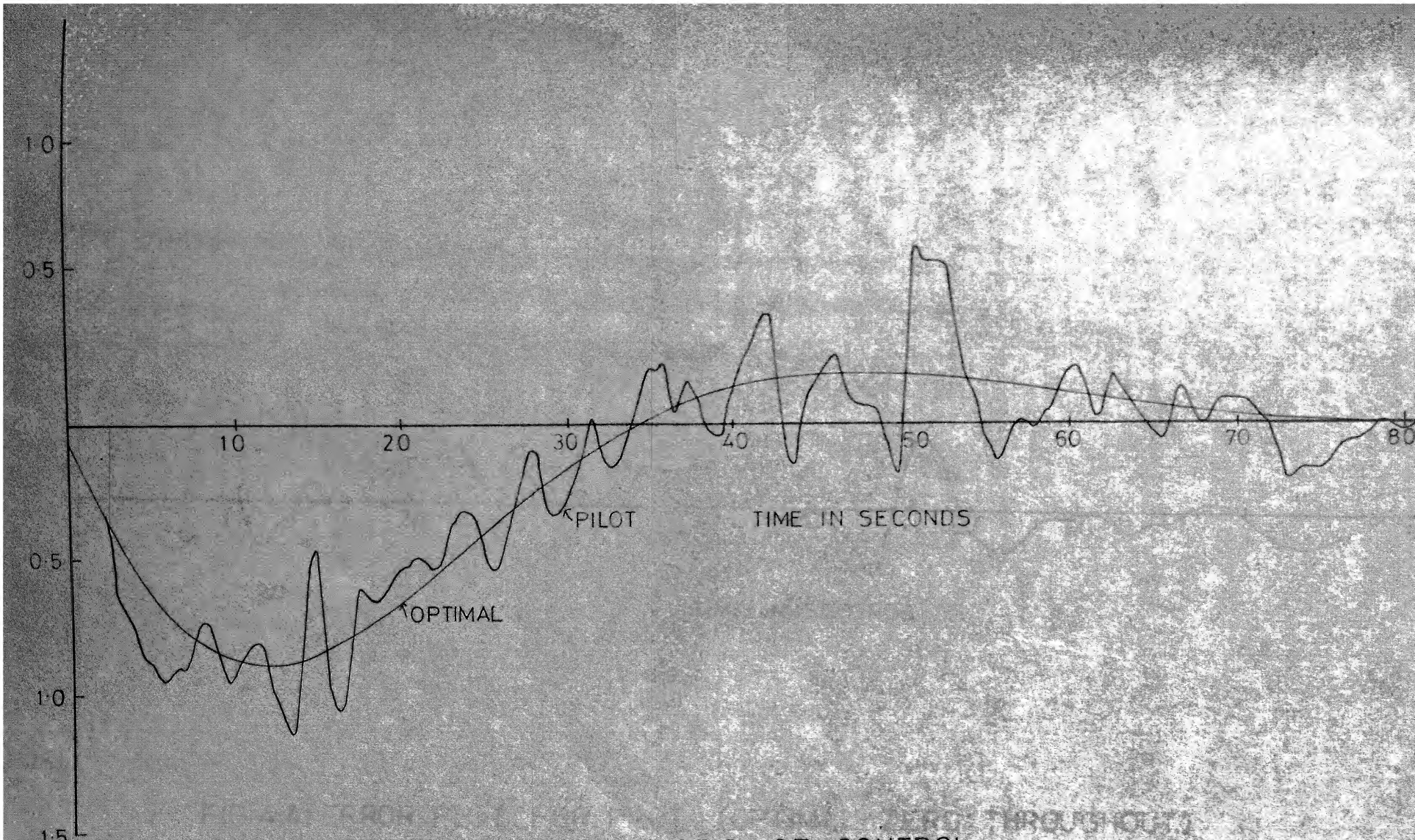

FIG.4·3: PLOTS OF CONTROL

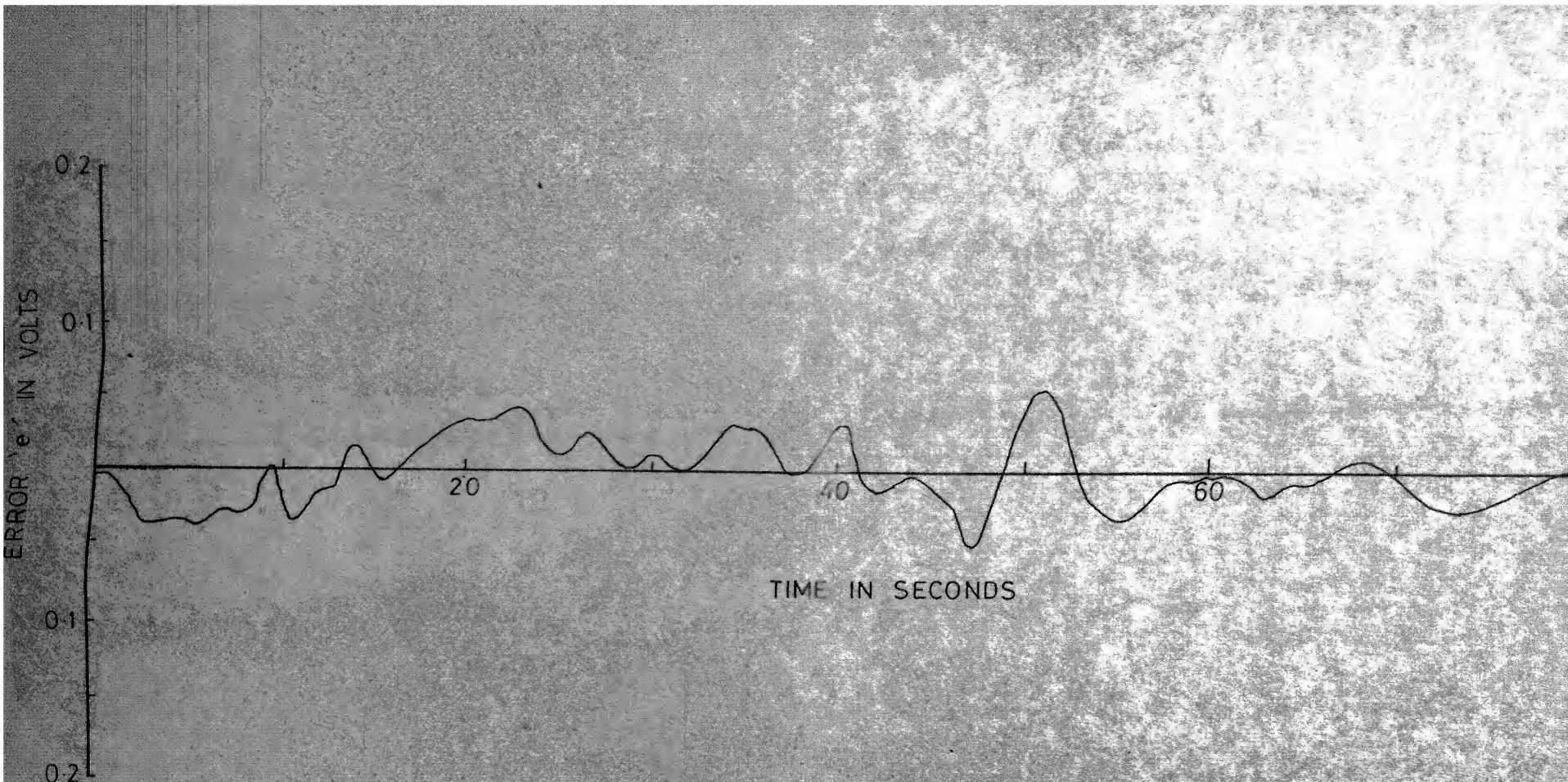

FIG.4·4: ERROR PLOT FOR PILOT (OPTIMAL-ZERO THROUGHOUT)

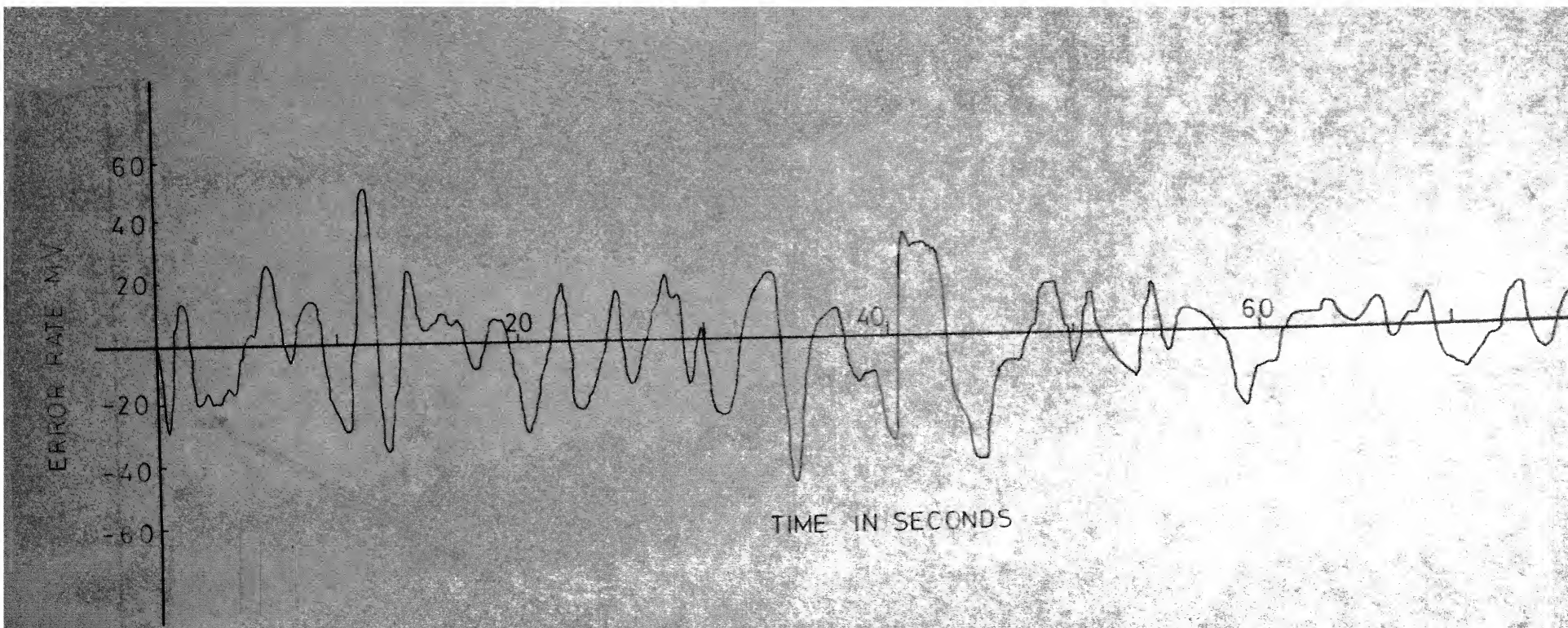

FIG. 4.5: ERROR RATE PLOT FOR PILOT (OPTIMAL- ZERO THROUGHOUT)

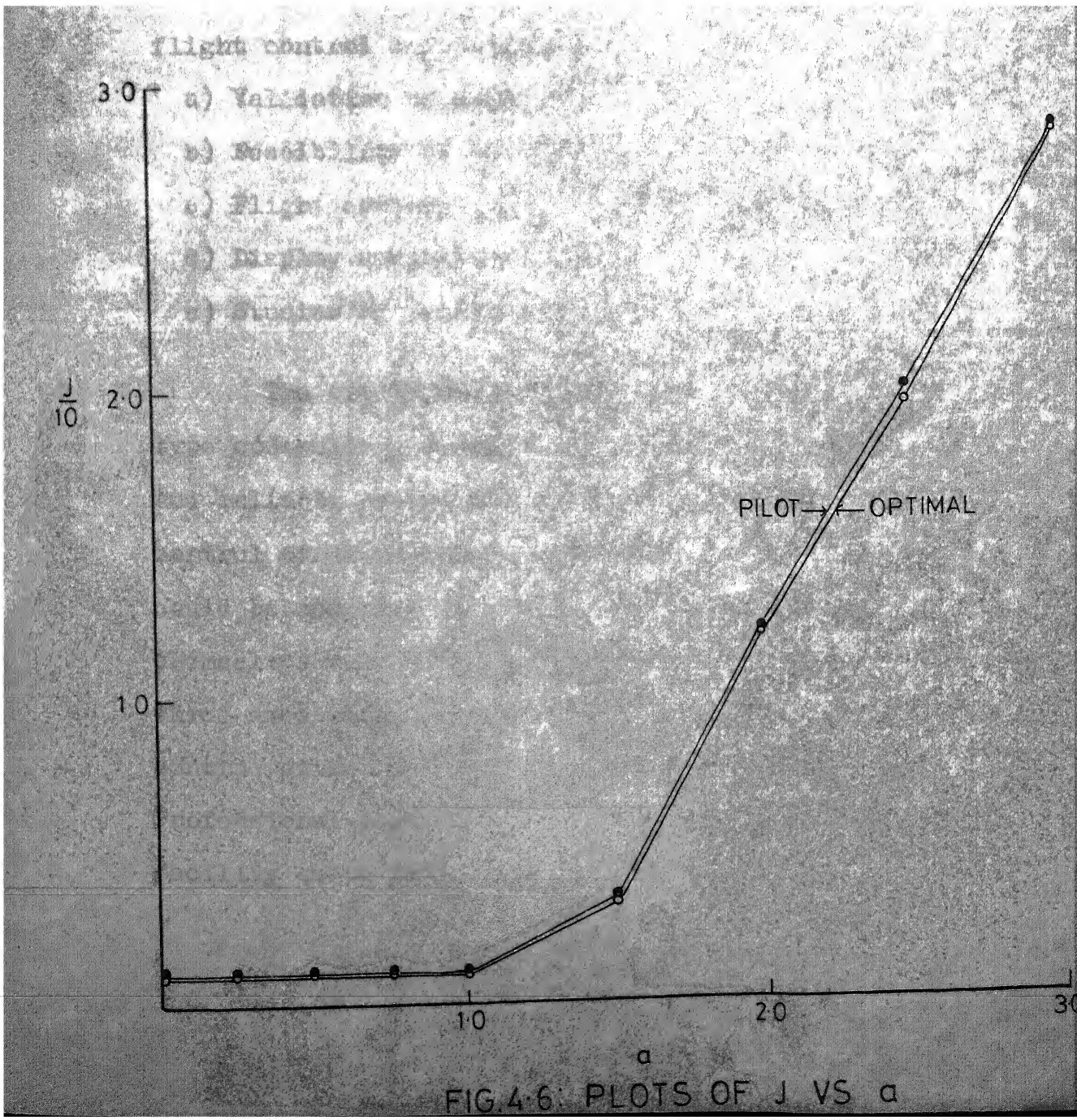

FIG.4.6: PLOTS OF J VS α

CHAPTER 5

CONCLUSIONS

5.1 SUMMARY

A typical rudimentary flight simulation facility assembled was described in the thesis, along with the illustrative case studies that were performed. Within the resources available effort was made to incorporate the essential features required for performing a range of flight control and allied studies like

a) Validation of human pilot models.

b) Feasibility of new flight control techniques

c) Flight control system comparison studies.

d) Display comparison studies

e) Studies of preliminary part designs of aircraft.

The simulation facility had an acceptable aircraft type controller, a modest but versatile analog computer and reliable performance recorders. With the throttle and control stick provided, a reasonable measure of realism could be achieved in pitching movements. However, the two themselves were sufficient to effect symbolic controls in three axes using throttle for longitudinal movement and the control stick for vertical and lateral movements. Professional pilots who used the simulator found the facility quite satisfactory.

Two meaningful studies were performed on the facility. The first was a display optimisation study for aerial combat. State vector displays, predicted/quickened vector displays and control vector displays were tried out in assessing the performance of professional fighter pilots against an optimal solution available in literature developed through differential game theoretic techniques. The control vector display indicated most efficient performance but involved the pilot rather blindly taking away his initiative to correct even for system errors. The predictive displays were next best. Due to analog computer errors the exact type of predictive display could not be decided upon. This study revealed the defeciencies in system. The errors in analog elements at low voltage ranges of the parameters became comparable to that of the parametric signals themselves. This lead to erroneous system outputs.

The second study performed was an attempt to validate and use an optimal control theoretic pilot model. The model had been developed for deterministic inputs and a controlled element transfer function of the type $\frac{k_c}{s(s+a)}$. The performance of the optimal controller and an experienced Air Force pilot were compared over a series of flight simulated runs with varying plant damping ratios. The transfer function representation of the model was reasonably close to the quasilinear model developed by Mcruer using random inputs. It was also found that the

variation in the performance index of the optimal control model for different aircraft pitch damping ratios could be used as a guide in choosing the value for pitch damping of the aircraft.

5.2 SUGGESTED IMPROVEMENTS

a) Provision of rudder control would be essential to give completeness in controller realism. Flight control problems in all three dimensions could then be simulated realistically.

b) A hybrid computation facility using the available 'onlline digital system IBM 1820' and the analog system 'TR 20' would be desirable. This would enable simulation of problems with more complexity. The limited resources in TR 20 and its accuracy cramped the level of problems that could be tackled with the present set up.

5.3 SCOPE FOR FUTURE STUDIES

a) An interesting addition in the display optimisation study could be the display of a combination of state vectors, quickened vectors and control vectors. A facility for selection of the different displays by the pilot at will as well as a possible change of scale of each display could indeed improve the overall performance of the pilots. These could be tried out after incorporating the improvements in computation facility as suggested above.

b) The investigations on the optimal control theoretic pilot model could be extended further using

random inputs. Currently more involved optimal control models considering the 'Human pilot as an optimal controller and information processor' are being developed.[19] Validation studies of these could be taken up.

c) There are a host of optimal manoeuvre solutions in flight, available in the literature like the minimum time turns and climbs for supersonic aircraft. These would constitute interesting studies on the simulator.

It would thus be seen that a flight simulator, would indeed be a handy tool in verifying various results in flight control and investigating with piloted simulator runs, preliminary designs of aerospace machines which are vital for the continued human achievement in aerospace field.

APPENDIX A

TR 20 DETAILED SPECIFICATIONS[10]

Element	Specifications
1. General	Voltage: 10V d.c. Power: 60 watts
2. D.C. Amplifier	Output voltage range: ±10V Noise from d.c. to 500 Kc: 200 uV max. Offset at summing junction: 20 uV max.
3. Integrators	Accuracy: Typical 100% ± 0.1% Minimum 100% ± 0.2% Driftrate: 20 mV/sec. typical 50 uV/sec. typical
4. Quarter Square Multiplier	Input voltage range: -10V to +10V Output voltage range: -10V to +10V Static error: 40 mV nominal 80 mV maximum
5. X^2 Diode Function Generator (X^2 DFG)	Input voltage range: 0 to ± 10 V Error: typical 0.2% maximum 0.4%
6. Log X DFG	Input voltage: 0.1 to 10V Output voltage: 1 to 10V Static error: Maximum ±1% full scale Nominal 0.5% full scale.

APPENDIX B

CONVERSION OF PROBLEM EQUATIONS TO SUIT ANALOG SIMULATION IN DISPLAY OPTIMISATION STUDY

The problem equations are

$$\ddot{r}(t) = a_p - a_e \tag{B.1}$$

$$\hat{\dot{r}}(t) = (a_p - a_e)\, T-t \tag{B.2}$$

$$\hat{\hat{r}}(t) = \hat{r}(t) + (a_p - a_e)\,\frac{(T-t)^2}{2} \tag{B.3}$$

$$a^*_{p(c)} = -\frac{E_{p(c)}(t)}{\sqrt{\frac{T-t}{3}}}\;\frac{\hat{r}(t)}{\|\hat{r}(t)\|} \tag{B.4}$$

$$E^2_{p_{(e)}}(t) = E^2_{p(e)}(t_o) - \int_{t_o}^{t} \left\{a_{p(e)}(t)\; a_{p(e)}(t)\right\} dt \tag{B.5}$$

* are assumed implicit in all the equations.

Resolving (B.4) into x and y coordinates

$$a_{p(e)_x} = -\frac{E_{p(e)}(t)}{\sqrt{\frac{T-t}{3}}}\;\frac{\hat{r}_x(t)}{\|\hat{r}(t)\|} \tag{B.6}$$

$$a_{p(e)_y} = -\frac{E_{p(e)}(t)}{\sqrt{\frac{T-t}{3}}}\;\frac{\hat{r}_y(t)}{\|\hat{r}(t)\|} \tag{B.7}$$

Now

$$a_{p(e)}(t)\cdot a_{p(e)}(t) = a^2_{p(e)_x}(t) + a^2_{p(e)_y}(t)$$

$$= \frac{3E^2_{p(e)}(t)}{T-t}\cdot\frac{\hat{r}^2_x + \hat{r}^2_y}{\|\hat{r}(t)\|^2}$$

or $$a_{p(e)}(t)\cdot a_{p(e)}(t) = (3E^2_{p(e)})/(T-t) \tag{B.8}$$

Using (B.8) in (B.5)

$$E_p^2(t) = E_p^2(t_o) - \int_{t_o}^{t} \frac{3E_p^2(t)}{(T-t)}\, dt$$

This we recognise as the solution of the differential equation.

$$\dot{E}_p^2(t) = -3\,\frac{E_p^2(t)}{T-t} \qquad (B.9)$$

or

$$\dot{E}_p(t) = -\frac{3}{2}\,\frac{E_p(t)}{T-t} \qquad (B.10)$$

Similarly

$$\dot{E}_e(t) = -\frac{3}{2}\,\frac{E_e(t)}{T-t} \qquad (B.11)$$

Dividing (B.10) by (B.11)

$$\frac{dE_p/dt}{dE_e/dt} = \frac{E_p(t)}{E_e(t)} \quad \text{or} \quad \frac{dE_p}{E_p} = \frac{dE_e}{E_e}$$

Integrating $\log E_p = \log E_e + \log C$

$$\text{or} \quad \frac{E_p(t)}{E_e(t)} = \frac{E_p(t_o)}{E_e(t_o)} = C \qquad (B.12)$$

Now substituting (B.4) in (B.2)

$$\dot{\hat{r}}(t) = \sqrt{3(T-t)}\,\frac{\hat{r}(t)}{\|\hat{r}(t)\|}\,(E_e(t) - E_p(t)) \qquad (B.13)$$

Resolving (B.13) into x and y coordinates,

$$\dot{\hat{r}}_x(t) = \sqrt{3(T-t)}\,\frac{\hat{r}_x(t)}{\|\hat{r}(t)\|}\,(E_e(t) - E_p(t)) \qquad (B.14)$$

$$\dot{\hat{r}}_y(t) = \sqrt{3(T-t)}\ \frac{\hat{r}_y(t)}{\|\hat{r}(t)\|}\,(E_c(t) - E_p(t)) \qquad \text{(B.15)}$$

Dividing (B.15) by (B.14) and integrating

$$\frac{\hat{r}_y(t)}{\hat{r}_x(t)} = \frac{\hat{r}_y(t_o)}{\hat{r}_x(t_o)} = k \qquad \text{(B.16)}$$

$$\|\hat{r}(t)\| = \left[\hat{r}_x^2(t) + \hat{r}_y^2(t)\right]^{\frac{1}{2}}$$

$$= \left[\hat{r}_x^2(t)\ (1+k^2)\right]^{\frac{1}{2}}$$

or $$\|\hat{r}(t)\| = \hat{r}_x(t)\sqrt{1+k^2}$$

Using this in (B.14), we get

$$\dot{\hat{r}}_x(t) = \sqrt{3/(1+k^2)}\cdot\left(\frac{1}{C} - 1\right) E_p(t)\sqrt{T-t} \qquad \text{(B.17)}$$

$$\hat{r}_y(t) = k\,\hat{r}_x(t) \qquad \text{(B.18)}$$

Similar manipulation on (B.4) yields

$$a_{p_x}(t) = -\sqrt{\frac{3}{1+k^2}}\ \frac{E_p(t)}{\sqrt{T-t}} \qquad \text{(B.19)}$$

$$a_{p_y}(t) = k\,a_{p_x}(t) \qquad \text{(B.20)}$$

Using (B.19) and (B.12) in (B.1) and simplifying,

$$\ddot{r}_x(t) = a_{p_x}(t)\ \left(1 - \frac{1}{C}\right) \qquad \text{(B.21)}$$

$$\ddot{r}_y(t) = a_{p_x}(t)\ \left(k - \frac{k}{C}\right) \qquad \text{(B.22)}$$

Resolving (B.3) into x and y coordinates

$$\hat{\hat{r}}_x(t) = \hat{r}_x(t) - (a_{p_x} - a_{e_x}) \frac{(T-t)^2}{2} \qquad \text{(B.23)}$$

and

$$\hat{\hat{r}}_y(t) = \hat{r}_y(t) - (a_{p_y} - a_{e_y}) \frac{(T-t)^2}{2} \qquad \text{(B.24)}$$

Dividing (B.24) by (B.23)

$$\frac{\hat{\hat{r}}_y(t)}{\hat{\hat{r}}_x(t)} = \frac{\hat{\hat{r}}_y(t_o)}{\hat{\hat{r}}_x(t_o)} = k \qquad \text{(B.25)}$$

Thus the equations for final simulation of optimal solution on analog computer would be

$$\dot{E}^2_{p(o)}(t) = -3 \frac{E^2_p(t)}{T-t} \qquad \text{(B.26)}$$

$$\dot{\hat{r}}_x(t) = \sqrt{\frac{3}{1+k^2}} \left(\frac{1}{C} - 1\right) E_p(t) \sqrt{T-t} \qquad \text{(B.27)}$$

$$\hat{r}_y(t) = k\, \hat{r}_x(t) \qquad \text{(B.28)}$$

$$\ddot{r}_x(t) = a_{p_x}(t) \left(1 - \frac{1}{C}\right) \qquad \text{(B.21)}$$

$$\ddot{r}_y(t) = a_{p_x}(t) \left(k - \frac{k}{C}\right) \qquad \text{(B.22)}$$

$$\hat{\hat{r}}_x(t) = \hat{r}_x(t) - (a_{p_x} - a_{e_x}) \frac{(T-t)^2}{2} \qquad \text{(B.23)}$$

$$\hat{\hat{r}}_y(t) = k\, \hat{\hat{r}}_x(t) \qquad \text{(B.27)}$$

$$a_{p(o)_x}(t) = -\sqrt{\frac{3}{1+k^2}} \frac{E_{p(o)}(t)}{\sqrt{(T-t)}} \qquad \text{(B.19)}$$

$$a_{p(o)_y}(t) = k\, a_{p(e)_x}(t) \qquad \text{(B.20)}$$

APPENDIX C

EQUATIONS FOR OPTIMUM ANALOG REALISATION OF SADDLE POINT SOLUTIONS

Solving equation (B.10) analytically,

$$\frac{dE_p(t)}{dt} = -1.5 \frac{E_p(t)}{T-t} \quad ; \quad E_p(t_o) = E_{p_o}$$

$$\frac{dE_p(t)}{E_p(t)} = -\frac{1.5}{T-t}\, dt$$

Integrating $\ln(E_p(t)) = \ln C(T-t)^{1.5}$

or $\quad E_p(t) = C\,(T-t)^{1.5}$

Using boundary condition,

$$E_p(t_o) = C\,T^{1.5}$$

$$C = E_{p_o}\, T^{-1.5}$$

Hence

$$E_p(t) = E_{p_o}\left(\frac{T-t}{T}\right)^{1.5} \qquad (C.1)$$

Substituting this in (B.19) we get

$$a_{p_x}(t) = -\sqrt{\frac{3}{1+k^2}}\, \frac{E_{p_o}}{\sqrt{(T-t)^{3}}} \left(\frac{(T-t)}{T}\right)^{1.5}$$

$$= -\sqrt{\frac{3}{1+k^2}}\, \frac{E_{p_o}}{T^{1.5}}\, (T-t)$$

or

$$a_{p_x}(t) = - C_1 . C_2 (T-t) \qquad (C.2)$$

where

$$C_1 = \frac{E_{p_o}}{T^{1.5}} \quad \text{and} \quad C_2 = \sqrt{\frac{3}{1+k^2}}$$

Similarly

$$a_{e_x}(t) = -\sqrt{\frac{3}{1+k^2}} \cdot \frac{E_{e_o}}{T^{1.5}} (T-t)$$

$$= -C_2 . C_1 \cdot \frac{1}{C}(T-t)$$

Hence

$$\ddot{r}_x = a_{p_x} - a_{e_x}$$

$$= -C_1 . C_2 (1 - \frac{1}{C})(T-t) \qquad (C.3)$$

Now

$$\dot{\hat{r}}_x = \ddot{r}_x (T-t)$$

$$= -C_1 . C_2 (1 - \frac{1}{C}) (T-t)^2 \qquad (C.4)$$

Hence the optimised equations for analog mechanisation would be

$$\dot{E}_p^2 = -3 \frac{E_p^2}{T-t} \qquad (C.5)$$

$$a_{p_x} = -C_1 . C_2 (T-t); \quad a_{p_y} = k\, a_{p_x} \qquad (C.6)$$

$$\dot{\hat{r}}_x = -C_1 \cdot C_2\left(1 - \frac{1}{C}\right)(T-t)^2; \quad C = \frac{E_{p_o}}{E_{e_o}} \tag{C.7}$$

$$\hat{r}_y = k\, \hat{r}_x \tag{C.8}$$

$$\hat{\hat{r}}_x = r_x - C_1 \cdot C_2\left(1 - \frac{1}{C}\right)(T-t) \tag{C.9}$$

$$\hat{\hat{r}}_y = k\, r_x \tag{C.10}$$

$$\dot{r}_x = -C_1 \cdot C_2\left(1 - \frac{1}{C}\right)(T-t) \tag{C.11}$$

$$\ddot{r}_y = -C_1 \cdot C_2\left(k - \frac{k}{C}\right)(T-t) \tag{C.12}$$

APPENDIX D

ANLOG SETUP FOR OPTIMAL SOLUTION

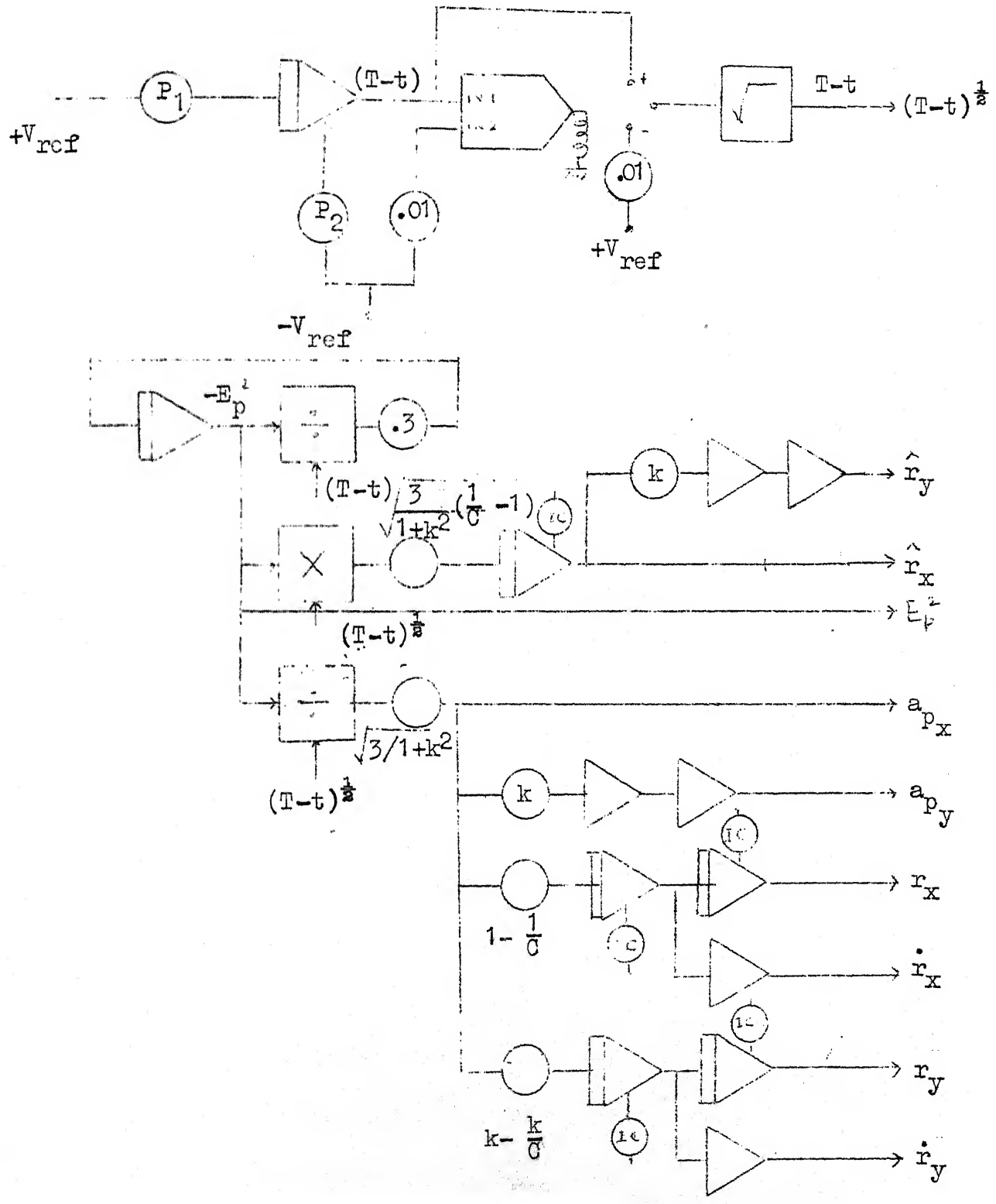

APPENDIX E

ANALOG SETUP WITH PILOT IN LOOP

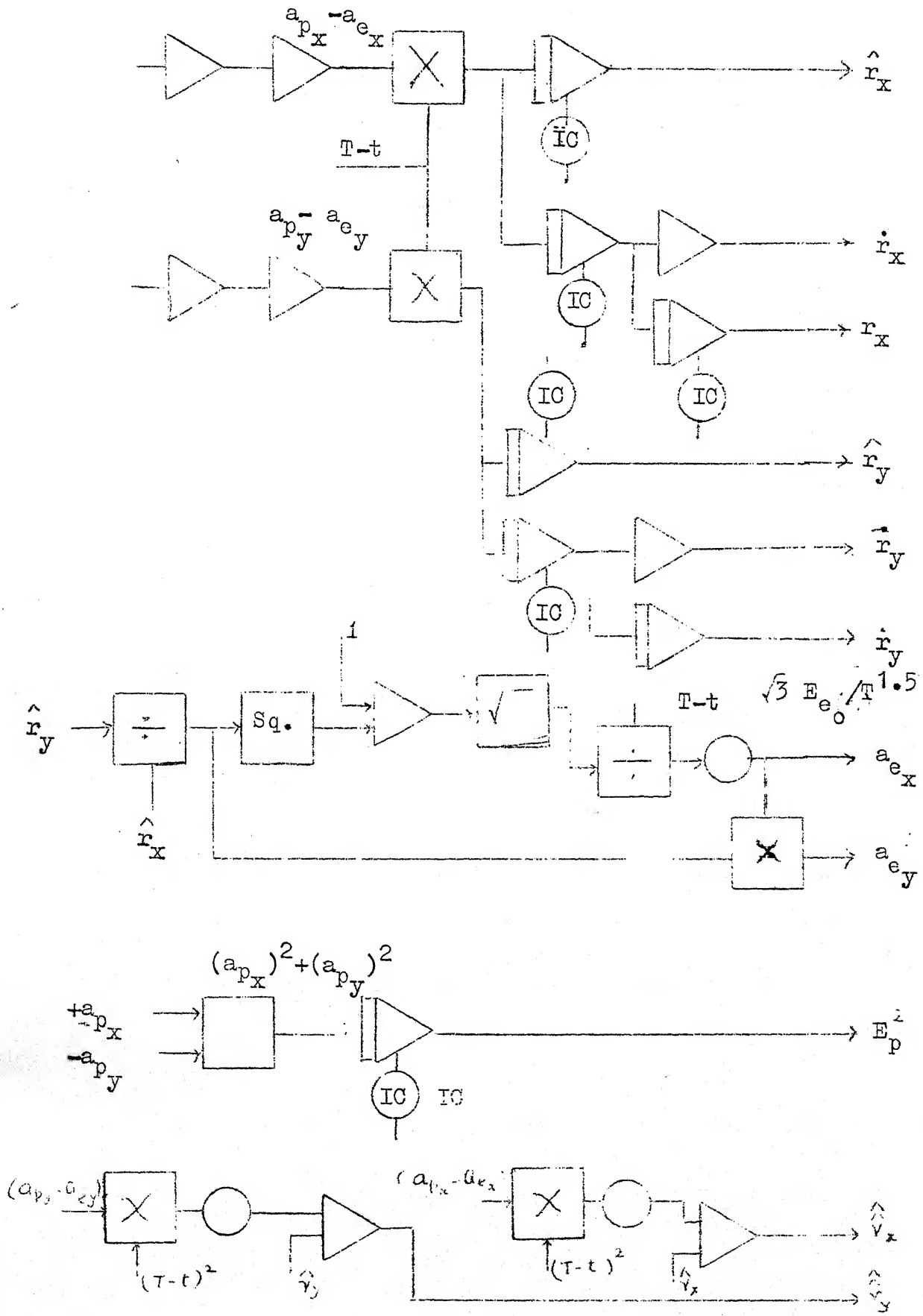

ANALOG SETUP FOR PILOT MODEL STUDY

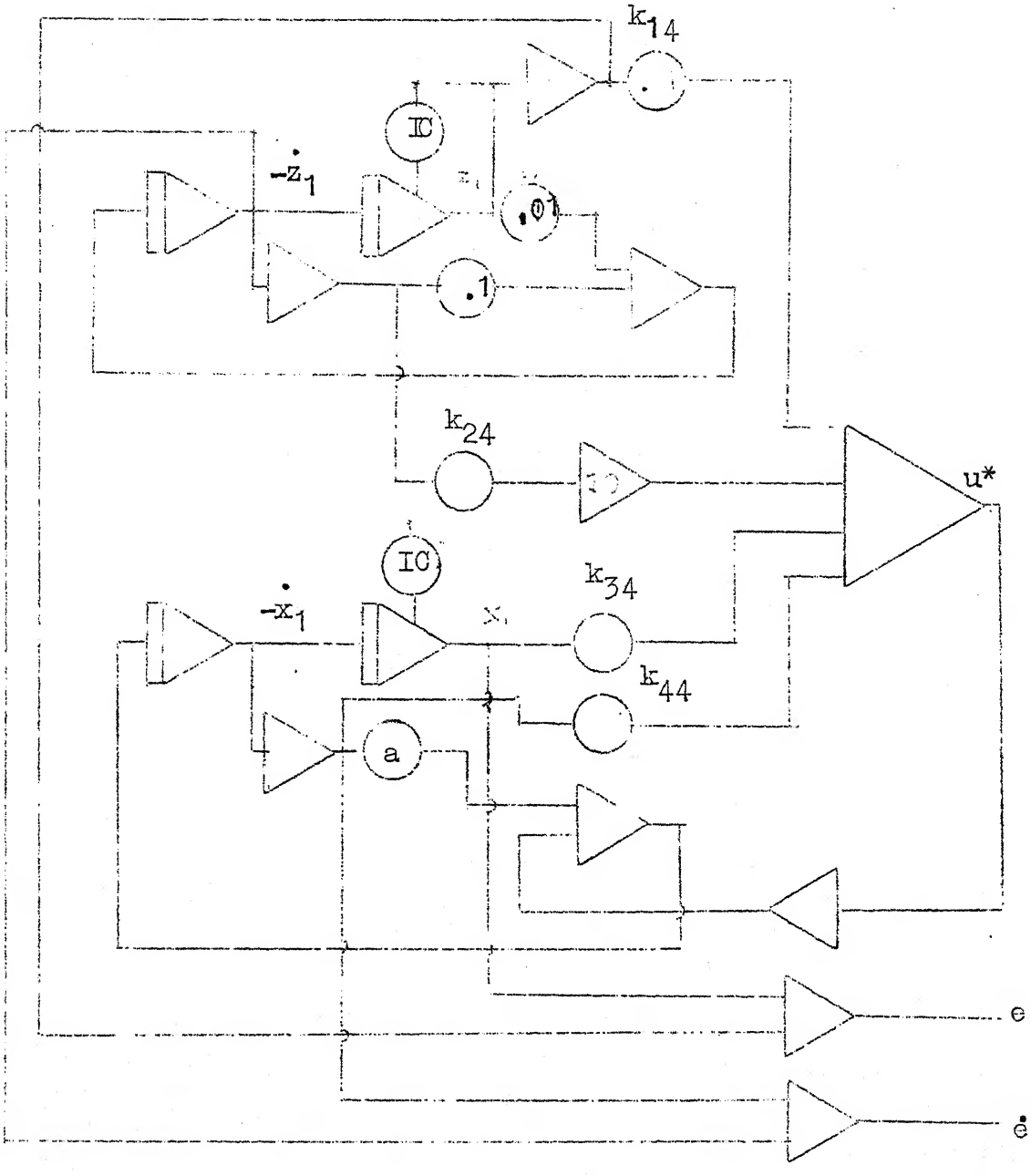

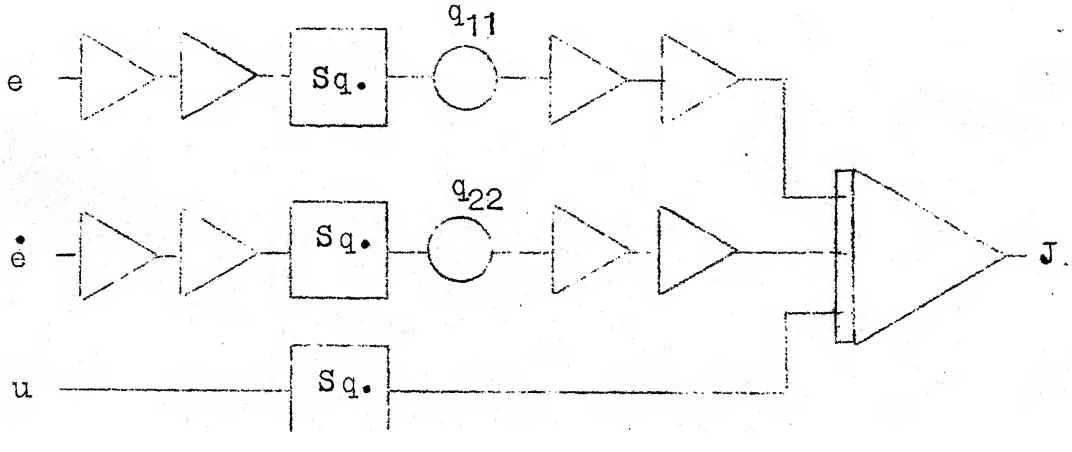

REFERENCES

1. Steven, E. Belsley, "Man Machine System Simulation for Flight Vehicles", IEEE Transactions on Human Factors in Electronics, Vol.HFE-4, No.1, Sept.196

2. R.W. Obermeyer and F.A. Muckler, "Performance Measurement in Flight Simulation Studies", AIAA Simulation for Aerospace Flight Conference, August 1963.

3. R.W. Obermeyer and F.A. Muckler, "Modern Control System Theory and Human Control Functions", Proc. of the Fifth National Symposium on Human Factors in Electronics, May 1964.

4. F.W. Prillman,W.W.Huff,Jr.& J.T.Hooks Jr., "A Manned Air to Air Combat Simulator", Journal of Aircraft, Vol. 6, No.4, August 1969.

5. John Deshon Warner, "Evaluation of a New Aircraft Controller Concept for the SST", Fifth Annual NASA University Conference on Manual Control, 1969.

6. Classified Air Publications No.

7. Classified Air Publication No. 4951.

8. Relevant Indian Air Force Notes for pilots.

9. R. Feifer, R. Smith and R. Westerman, "Joysticks - An Old Tool with New Uses", Proc. of Fifth National Symposium on Human Factors in Electronics, 1964.

10. PACE-TR 20 Maintenance Manual; Electronic Associates Incorporated, New Jersey, USA.

11. Y.C. Ho, A.E. Bryson Jr. and S. Baron, "Differential Games and Optimal Pursuit Evasion Strategies", IEEE Transactions on Automatic Control, AC-10,No.4, October 1965.

12. S. Baron, "Differential Games and Manual Control", IEEE Transactions on Human Factors in Electronics, HFE-7, No.4, December 1966.

13. John Deshon Warner, "Manual Control System Performance with Predictive Displays", Fourth Annual NASA University Conference on Manual Control, 1968.

14. Gary L.Blank and Peter J. Schumacher, Jr., "The Human Operator as an Optimal Controller", Proc. of Sixth Annual Allerton Conference on Circuit andSSystem Theory, 1968.

15. M.S. Krishnamoorthy,"Optimal Control Theoretic Validation of Handling Qualities Criteria," M.Tech.Thesis, 1971, Indian Institute of Technology, Kanpur.

16. I.G. Sarma, "Lectures on Flight Control and Handling Qualities Problem", Book.

17. Duane T.Mcruer and Henry R. Jex, "A Review of Quasilinear Pilot Models", IEEE Transaction on Human Factors in Electronics, VolHFE-8, No.3, September 1967.

18. T.E. Lollar, "A Rationale for the Determination of Certain VTOL Handling Qualities Criteria", AGARD Report No.471, July 1963.

19. S. Baron and David L. Kleinman, "Human Operator as an Optimal Controller and Information Processor", Fourth Annual NASA University Conference on Manual Control, 1968.

EE-1972-M-SES-FLI